PERGAMON

International Journal of Solids and Structures 38 (2001) 5421–5451

INTERNATIONAL JOURNAL OF SOLIDS and STRUCTURES

www.elsevier.com/locate/ijsolstr

# Elastoplastic-damage modelling including the gradient of damage: formulation and computational aspects

B. Nedjar *

*Laboratoire d'Analyse des Matériaux et Identification, Ecole Nationale des Ponts et Chaussées, ENPC-LAMI, 6 et 8, Avenue Blaise Pascal, Cite Descartes, 77455 Marne la Vallée Cedex 2, France*

Received 26 July 1999

**Abstract**

A framework for continuum elastoplastic-damage modelling, which employs irreversible thermodynamics and internal state variables, is investigated. The damage part of the modelling involves the gradient of damage quantity which, together with the equations of motion, are issued from a new formulation of the principle of virtual power recently proposed. It is shown how the plastic part of the modelling takes its standard format. Next, we consider in detail the variational formulation and subsequent numerical implementation of the elastoplastic-damage models. The development of an algorithm consistent with the present formulation is given where, for the plastic part, it leaves the standard return mapping algorithms unchanged. Application is made to different classical rate-independent and rate-dependent plastic models with the presence of a damage mechanism. The numerical implementation in the context of the finite element method is discussed in detail and a set of representative applications and numerical examples is given. 

*Keywords:* Continuum damage mechanics; Gradient of damage; Coupling with elastoplasticity; Continuum thermodynamics; Finite element method

## 1. Introduction

Continuum damage theories are based on the thermodynamics of irreversible processes where damage is described by internal quantities. Isotropic damage formulations are extensively employed in the literature because of their simplicity, efficiency and adequacy for many practical applications. The formalism and the evolution equations for the damage modelling part used in this paper are issued from a new formulation of the principle of virtual power recently proposed in Frémond and Nedjar (1993, 1996) and Nedjar (1995).

Damage in a solid results from microscopic movements. In this theory, it is decided to take into account the power of these microscopic movements in the power of the internal forces. This latter is chosen to depend, besides on the strain rates, also on the damage rate which is clearly related to the microscopic movements. Furthermore, it is assumed that it depends also on the gradient of the damage rate to account

* Fax: +33-1-64-15-37-41.
*E-mail address:* nedjar@lami.enpc.fr (B. Nedjar).

0020-7683/01/$ - see front matter 
PII: S0020-7683(00)00358-9

for the microscopic interactions between the material points, i.e. to take into account the influence of damage at a material point on the damage of its neighbourhood. As shown in Frémond and Nedjar (1996) and Nedjar (1995), the elastic-damage models issued from this formulation are free of spurious mesh sensitivity.

The aim of this work is to include the plastic modelling within the framework of the above formalism. Part of the ideas presented in this paper have been briefly outlined in Nedjar (1999b). From the theoretical point of view, and consistent with thermodynamic requirements, it is shown that this coupling between damage and plasticity is treated naturally with a simple adequate choice of the dissipation function. The straightforward use of the *Legendre* transform to get the conjugate of this last function leads to two yield criteria. The first one is related to damage, and the second one is the one used in classical plasticity. The elastoplastic-damage formulation obtained is then characterized by the following facts:

- a simple coupling between damage and elastoplasticity,
- the plastic part takes its standard format, i.e. additive decomposition of the strain, constitutive relation, yield function, flow rule and the Kuhn–Tucker loading/unloading conditions,
- the formulation is independent of the particular types of the plastic and damage evolution parts of the models,
- models characterized by a rate-dependent damage and/or a rate-dependent plastic mechanisms are readily obtained through adequate modifications of their inviscid counterparts.

The variational formulation is considered in detail and the problem of numerically integrating the elastoplastic-damage constitutive equations in the context of the finite element method is addressed. Within a typical time interval, we propose an approximation of the evolution equations constructed via a product formula algorithm on the basis of a convenient operator split of the coupled problem. The resulting procedure takes then the form of an *Elastic-Damage predictor/Plastic corrector* scheme. The algorithm used for the *elastic-damage predictor* part is the one already used in Frémond and Nedjar (1996) and Nedjar (1995) for static problems and in Nedjar (1999a) for dynamic problems. For the *plastic corrector* part, return mapping is used where a simple coupling with damage is added. From the practical standpoint, the standard return mapping algorithms, see Ortiz and Simo (1986), Simo and Hughes (1998) and Simo and Taylor (1985) among others, remain unchanged.

The remainder of the paper is organized as follows: first, a brief description of the damage theory we use is given. Then, as a point of departure, a rate-independent/rate-dependent elastic-damage model is outlined to make matters as concrete as possible. In Section 4, the elastoplastic-damage modelling framework is addressed in detail. In Section 5, we consider in detail the variational formulation and address the formal steps involved in the numerical implementation of the models within the framework of the finite element method. In Section 6, a set of representative numerical examples is presented where application is made to different classical rate-independent plastic models with the presence of a damage mechanism. Also, we show in Section 6.4, and through a model example, how the extension is made to incorporate rate-dependent damage and rate-dependent plasticity. And finally, conclusions are drawn in Section 7. Noteworthy remarks and comments are given throughout this paper.

## 2. Equations of motion and constitutive laws

In this section, the formulation of the damage theory we use is recalled. For a complete treatment, we refer to Frémond and Nedjar (1993, 1996) and Nedjar (1995).

Let the scalar $\beta(\mathbf{x}, t)$ be a damage quantity with value 1 when the material is undamaged and value 0 when it is completely damaged. The basic idea of the theory we use is to modify the power of the internal forces.

Within the solid, there exist microscopic movements which produce damage. We think that the power of these microscopic movements must be taken into account. Thus, we choose the power of the internal forces to depend, besides on the strain rates, also on the damage rate and the gradient of damage rate. These latter quantities are clearly related to the microscopic movements. The gradient of damage is introduced to take into account the influence of damage at a material point on the damage of its neighbourhood.

### 2.1. Principle of virtual power and equations of motion

For a domain $\Omega$ with boundary $\partial\Omega$, we choose the power of the internal forces $P_{\mathrm{i}}$ as:

$$P_{\mathrm{i}}\left(\Omega, \mathbf{u}, \frac{\mathrm{d}\beta}{\mathrm{d}t}\right) = -\int_{\Omega} \boldsymbol{\sigma} : \mathbf{D}(\mathbf{u})\,\mathrm{d}\Omega - \int_{\Omega} \left(B\frac{\mathrm{d}\beta}{\mathrm{d}t} + \mathbf{H}\cdot\operatorname{grad}\frac{\mathrm{d}\beta}{\mathrm{d}t}\right)\mathrm{d}\Omega, \tag{1}$$

where $\boldsymbol{\sigma}$ is the stress tensor and $\mathbf{D}(\mathbf{u})$ is the strain rates tensor ($\mathbf{u}$ being the macroscopic velocity). The two non-classical quantities are: $B$, the internal work of damage (dual to $\beta$) and $\mathbf{H}$, the flux vector of internal work of damage (dual to $\operatorname{grad}\beta$).

While the power of the external forces $P_{\mathrm{e}}$ takes its classical expression, we choose the power of the acceleration forces $P_{\mathrm{a}}$ as:

$$P_{\mathrm{a}}\left(\Omega, \mathbf{u}, \frac{\mathrm{d}\beta}{\mathrm{d}t}\right) = \int_{\Omega} \rho\frac{\mathrm{d}\mathbf{u}}{\mathrm{d}t}\cdot\mathbf{u}\,\mathrm{d}\Omega + \int_{\Omega} \underline{\rho}\frac{\mathrm{d}^2\beta}{\mathrm{d}t^2}\frac{\mathrm{d}\beta}{\mathrm{d}t}\mathrm{d}\Omega, \tag{2}$$

where $\rho$ is the (volumetric) density. The quantity $\underline{\rho}(\mathrm{d}^2\beta/\mathrm{d}t^2)$ stands for the acceleration forces of the microscopic links; $\underline{\rho}$ being proportional to their mass with units ($\mathrm{kg\,m^{-1}}$), i.e. a linear mass density. As in Nedjar (1999a), one can choose for the applications to relate $\rho$ and $\underline{\rho}$ by taking $\underline{\rho} = \alpha\rho$, where $\alpha$ is only a convenient material parameter with dimensions ($\mathrm{m^2}$), and which can be zero valued if we decide to neglect the inertia effects of the microscopic movements.

The principle of virtual power gives then two sets of equations of motion:

$$\operatorname{div}\boldsymbol{\sigma} + \mathbf{f} = \rho\frac{\mathrm{d}\mathbf{u}}{\mathrm{d}t} \quad \text{in } \Omega, \qquad \boldsymbol{\sigma}\cdot\mathbf{n} = \mathbf{F} \quad \text{on } \partial\Omega, \tag{3}$$

$$\operatorname{div}\mathbf{H} - B = \alpha\rho\frac{\mathrm{d}^2\beta}{\mathrm{d}t^2} \quad \text{in } \Omega, \qquad \mathbf{H}\cdot\mathbf{n} = 0 \quad \text{on } \partial\Omega, \tag{4}$$

where div is the divergence operator and $\mathbf{n}$ is the outward normal unit vector to $\Omega\cdot\mathbf{f}$ and $\mathbf{F}$ are the volumetric and surfacic external forces, respectively. The non-classical Eq. (4) were first derived in Frémond and Nedjar (1993), see also Frémond and Nedjar (1996) and Nedjar (1995). They describe the damage evolution, i.e. the microscopic movements in the domain $\Omega$.

### 2.2. Thermodynamic basis and constitutive laws

Within the framework of continuum thermodynamics, see Coleman and Noll (1963), Coleman and Gurtin (1967), Germain et al. (1983) and Lemaitre and Chaboche (1988) among others, the state of the material is characterized by its free energy $\Psi$. It is then natural to assume that $\Psi$ is a function of the (small) strain tensor $\boldsymbol{\epsilon}$, the damage quantity $\beta$, and the gradient of damage grad $\beta$, i.e $\Psi \equiv \Psi(\boldsymbol{\epsilon}, \beta, \operatorname{grad}\beta)$. Due to the choice made for the power of the internal forces (see Eq. (1)), and confining our attention to the purely mechanical theory, the Clausius–Duhem (reduced dissipation) inequality takes the form:

$$-\dot{\Psi} + \boldsymbol{\sigma} : \dot{\boldsymbol{\epsilon}} + B\dot{\beta} + \mathbf{H}\cdot\operatorname{grad}\dot{\beta} \geqslant 0, \tag{5}$$

for any admissible process. Here $(\cdot)$ denotes the time derivative. Assuming for instance that there are only dissipative phenomena with respect to damage (the plasticity will be considered later), we choose to split the

internal work of damage $B$ into a reversible part $B^{\mathrm{r}}$, and a dissipative part $B^{\mathrm{d}}$, i.e. $B = B^{\mathrm{r}} + B^{\mathrm{d}}$. By taking the time derivative of $\Psi$, substituting into Eq. (5) and making use of standard arguments, see Coleman and Noll (1963), Coleman and Gurtin (1967) and Germain et al. (1983), one obtains

$$\boldsymbol{\sigma} = \frac{\partial \Psi}{\partial \boldsymbol{\epsilon}}, \qquad \mathbf{H} = \frac{\partial \Psi}{\partial (\operatorname{grad} \beta)}, \qquad B^{\mathrm{r}} = \frac{\partial \Psi}{\partial \beta}, \tag{6}$$

and the dissipative inequality

$$B^{\mathrm{d}} \dot{\beta} \geqslant 0. \tag{7}$$

As in Moreau (1970), see also Germain et al. (1983), we postulate the existence of a pseudo-potential of dissipation $\Phi$, i.e. a positive, convex and sub-differentiable function with $\Phi(\dot{\beta} = 0) = 0$, such that

$$B^{\mathrm{d}} = \frac{\partial \Phi}{\partial \dot{\beta}}, \tag{8}$$

which suffices to satisfy the inequality (7) for any admissible process. Thus, the constitutive law for the internal work of damage is then given by

$$B = B^{\mathrm{r}} + B^{\mathrm{d}} = \frac{\partial \Psi}{\partial \beta} + \frac{\partial \Phi}{\partial \dot{\beta}}. \tag{9}$$

## 3. A rate-independent/rate-dependent damage model

The elastoplastic-damage modelling framework developed in this paper is independent of the particular choices of damage and plastic evolutions. However, to make matters as concrete as possible, we first start by giving an elastic-damage model within the framework of the theory outlined above. This model will serve as an example of application in what follows, i.e. it will be coupled with plastic models.

### 3.1. Outlines of the elastic-damage model

It is mainly observed that damage within a solid is produced by extensions when a certain threshold is achieved. Such a situation is observed in many rock-like materials such as concrete. Another characteristic of this material is its softening behaviour, i.e a gradual reduction of the load carrying capacity with increasing deformation.

As a model problem, we give here the rate-independent/rate-dependent damage model already proposed in Nedjar (1999a,b) (a variant of those proposed in Frémond and Nedjar (1993, 1996) and Nedjar (1995)).

The choices made for the free energy $\Psi$ and the pseudo-potential of dissipation $\Phi$ are as follows:

$$\Psi = \tfrac{1}{2}\beta \boldsymbol{\epsilon} : \mathbf{C} : \boldsymbol{\epsilon} + \tfrac{1}{2} k (\operatorname{grad} \beta)^2, \tag{10}$$

$$\Phi = \tfrac{1}{2} c \dot{\beta}^2 - \dot{\beta} \big\{ W + \tfrac{1}{2} \boldsymbol{\epsilon} : \mathbf{C} : \boldsymbol{\epsilon} - \beta^n S(\boldsymbol{\epsilon}) \big\} + I_{-}(\dot{\beta}), \tag{11}$$

with

$$S(\boldsymbol{\epsilon}) = \tfrac{1}{2} \Big[ 2\mu \boldsymbol{\epsilon}^{+} : \boldsymbol{\epsilon}^{+} + \lambda (\langle \operatorname{tr}[\boldsymbol{\epsilon}] \rangle^{+})^2 \Big], \tag{12}$$

and where tr denotes the trace operator and : denotes the double contracted product.

The first term in $\Psi \equiv \Psi(\boldsymbol{\epsilon}, \beta, \operatorname{grad} \beta)$ constitutes the simplest model where damage is coupled to elasticity. $\mathbf{C}$ is the classical symmetric rank four isotropic elasticity tensor at the undamaged state (with $\lambda$ and $\mu$ being the Lamé coefficients). In the second term, $k$ is a material parameter which measures the influence of

damage at a material point on the damage of its neighbourhood. It is expressed in terms of a volumetric energy multiplied by the square of an internal length, i.e. $((\mathrm{N\,m^{-2}})\,\mathrm{m^2})$.

In the expression of $\Phi \equiv \Phi(\dot{\beta};\beta,\boldsymbol{\epsilon})$, the state variables $\boldsymbol{\epsilon}$ and $\beta$ are considered as parameters. The quantity $W$ is the initial damage threshold expressed in terms of volumetric energy. The exponent $n$ is a material parameter that controls the hardening/softening behaviour of the material, with $n > 0$. It's role will be clear in the bifurcation analysis of the following Section 3.3.

$c$ is the viscosity parameter of damage expressed in terms of volumetric energy multiplied by time, $(\mathrm{N\,m^{-2}\,s})$. Note that in the literature, several models introduce rate-dependent constitutive relations. Besides on the physical motivations, the regularizing role of viscosity avoids the ill-posedness of the boundary value problem due to strain softening, as shown in Dubé et al. (1994), Needleman (1987) and Simo (1988) for example. However, rate-independent damage evolution can also be considered in our model. In fact, one can check that if $c = 0$, the function $\Phi$ is positively homogeneous of degree one.

In the expression of $S(\boldsymbol{\epsilon})$ (Eq. (12)) the function $\langle\cdot\rangle^+$ is the positive part of the scalar $\langle\cdot\rangle$. The positive part $\boldsymbol{\epsilon}^+$ of the strain tensor $\boldsymbol{\epsilon}$ is obtained after diagonalisation.

The function $I_-$ is the indicator function of the interval $]-\infty,0]$ ($I_-(x) = 0$, if $x \leqslant 0$, and $I_-(x) = +\infty$, if $x > 0$). With this function, the pseudo-potential of dissipation has its physical value for any actual or physical value of $\dot{\beta}$.

The motivation of the choice made for the expression of the pseudo-potential of dissipation $\Phi$ will be clear in the following Section 3.2.

Since the treatment of the transient dynamic problem plays no role in the developments that follow (we refer to Nedjar (1999a) for this treatment), we shall ignore inertia effects and confine our attention to the static case. By replacing the expressions (10) and (11) into first and second term of Eq. (6) and Eq. (9) one obtains the constitutive laws. In the domain $\Omega$, the equations of motion are then obtained by replacing the last results into Eqs. (3) and (4). We get then:

$$\begin{aligned} \mathrm{div}(\beta\mathbf{C} : \boldsymbol{\epsilon}) + \mathbf{f} = \mathbf{0} \quad & \text{in } \Omega, \\ \boldsymbol{\sigma}\cdot\mathbf{n} = \mathbf{F} \quad & \text{on } \partial\Omega, \end{aligned} \tag{13}$$

$$\begin{aligned} c\dot{\beta} - k\Delta\beta + \partial I_-(\dot{\beta}) \ni W - \beta^n S(\boldsymbol{\epsilon}) \quad & \text{in } \Omega, \\ k\tfrac{\partial\beta}{\partial\mathbf{n}} = 0 \quad & \text{on } \partial\Omega, \end{aligned} \tag{14}$$

where $\Delta$ is the Laplacian operator and $\boldsymbol{\sigma} = \beta\mathbf{C} : \boldsymbol{\epsilon}$ is the stress–strain relation.

Eq. (14) describe the damage evolution. The right hand side of first term of Eq. (14) is the source of damage governed by extensions (see the expression of $S(\boldsymbol{\epsilon})$ in Eq. (12)). The sub-differential (or generalized derivative) $\partial I_-(\dot{\beta})$ of $I_-(\dot{\beta})$ is a reaction which forces $\dot{\beta}$ to be negative or equal to zero ($\partial I_-(x) = \{0\}$ if $x < 0$ and $\partial I_-(0) = [0,+\infty[$).

**Remark 1.** In view of the stress–strain relation $\boldsymbol{\sigma} = \beta\mathbf{C} : \boldsymbol{\epsilon}$, and the fact that damage is governed by extensions (first term of Eq. (14)), i.e. an energy of positive strains, it is clear that the elastic-damage model exhibits dissymmetric behaviours between tension and compression. The threshold of damage in compression is greater than the one in tension. The degree of difference between these thresholds depends solely on the value of the Poisson's ratio $\nu$, i.e. the Poisson's effect. At the limit, if $\nu = 0$, there is no damage under simple compression tests. This is one of the reasons which guided the design of the present model in its primary versions Frémond and Nedjar (1993, 1996) and Nedjar (1995).

**Remark 2.** Following the comments made at the beginning of this section, the fact that $S(\boldsymbol{\epsilon})$ in Eq. (12) depends on positive strains is motivated by the observations made on rock-likes materials. However, for other materials where the damage mechanism could be indifferent from the sign of the strains, this partition (in Eq. (12)) is not necessary. On the other hand, the choice made for $S(\boldsymbol{\epsilon})$ is not unique. One can choose

alternative expressions in place of Eq. (12). For example, we can take $S(\boldsymbol{\epsilon}) = \mu^* \mathbf{e}^+ : \mathbf{e}^+$ where, $\mu^*$ is a material parameter ($\mu^* \equiv \mu$ for example) and $\mathbf{e} = \mathrm{dev}[\boldsymbol{\epsilon}]$ is the deviatoric strain tensor, to describe materials for which the damage process is more sensitive to shearing.

### 3.2. Alternative formulation of damage evolution

Further insight into the nature of the pseudo-potential of dissipation (11) is gained by examining its dual (conjugate) function. From Eq. (8), we have that:

$$B^{\mathrm{d}} = \frac{\partial \Phi(\dot{\beta})}{\partial \dot{\beta}} \quad \text{leads to} \quad \dot{\beta} = \frac{\partial \Phi^*(B^{\mathrm{d}})}{\partial B^{\mathrm{d}}}, \tag{15}$$

where $\Phi^*(B^{\mathrm{d}})$ is the *Legendre* transform (conjugate) of $\Phi(\dot{\beta})$ given by:

$$\Phi^*(B^{\mathrm{d}}) = \sup_{\dot{\beta}} \{\mathrm{B}^{\mathrm{d}} \dot{\beta} - \Phi(\dot{\beta})\}. \tag{16}$$

By replacing $\Phi$ by its expression in Eq. (11) and using the fact that $\frac{1}{2}\boldsymbol{\epsilon} : \mathbf{C} : \boldsymbol{\epsilon} = B^{\mathrm{r}}$ (by construction from third term of Eq. (6) and Eq. (10)), the identity (16) leads to:

$$\Phi^*(B^{\mathrm{d}}) = \sup_{\dot{\beta} \leqslant 0} \Big\{ -[\beta^n S(\boldsymbol{\epsilon}) - W - B]\dot{\beta} - \tfrac{1}{2} c \dot{\beta}^2 \Big\}, \tag{17}$$

where use of $B = B^{\mathrm{r}} + B^{\mathrm{d}}$ has been made. At this stage, and for clarity, the following two cases will be discussed separately: the rate-independent and the rate-dependent damage evolutions.

#### 3.2.1. Case $c = 0$: rate-independent damage evolution

For $c = 0$, the Legendre transform (17) leads to:

$$\Phi^*(B^{\mathrm{d}}) = I_{\{g = \beta^n S(\boldsymbol{\epsilon}) - W - B \leqslant 0\}}, \tag{18}$$

where $I_{\{\cdot\}}$ is the indicator function of the criterion $\{\cdot\}$, i.e., $\Phi^* = 0$ if $g \leqslant 0$ and $\Phi^* = +\infty$ if $g > 0$. This result leads then to the characterization of the state of damage by means of the damage criterion:

$$g = \beta^n S(\boldsymbol{\epsilon}) - W - B \leqslant 0. \tag{19}$$

The damage evolution (15) (second term) gives then:

$$\dot{\beta} = \dot{\delta} \frac{\partial g}{\partial B^{\mathrm{d}}} = \dot{\delta} \frac{\partial g}{\partial B} = -\dot{\delta}, \tag{20}$$

where $\dot{\delta} \geqslant 0$ is the so-called damage consistency parameter. The presence of the sign "$-$" in Eq. (20) is clear since the damage variable *decreases* from 1 to 0.

From first term of Eq. (4) in statics, one has $B = \mathrm{div}\,\mathbf{H}$. Furthermore, from second term of Eq. (6) and Eq. (10), $\mathbf{H} = k\,\mathrm{grad}\,\beta$ which leads to $B = k\Delta\beta$. Replacing this last result into Eq. (19) yields:

$$g = \beta^n S(\boldsymbol{\epsilon}) - W - k\Delta\beta \leqslant 0. \tag{21}$$

The present damage criterion (21) differs from classical (local) damage criterions with the presence of the term $-k\,\Delta\beta$. Note that this presence together with the boundary condition second term (or second term of Eq. (4)) ensures a well posed problem where the boundary condition is not postulated at the outset.

**Remark 3.** Classical local damage models can be recovered from the above formulation simply by taking $k = 0$ (or $\mathbf{H} = k\,\mathrm{grad}\,\beta = \mathbf{0}$). In particular, for our model, the criterion (21) becomes:

$$g = \beta^n S(\boldsymbol{\epsilon}) - W \leqslant 0, \tag{22}$$

which, together with Eq. (20) and the damage consistency condition $\dot{g} = 0$, leads to the damage flow rule:

$$\dot{\beta} = -\frac{\beta}{nS}\dot{S} \equiv \chi(S,\beta)\dot{S}. \tag{23}$$

A form identical to that proposed in Simo and Ju (1987a,b) for isotropic damage modelling, with the difference that here damage is governed by $S$, i.e, an energy of positive strains.

Observe that Eq. (22) can also be given in the form $g = S(\boldsymbol{\epsilon}) - (W/\beta^n) \leqslant 0$ which justifies the definition 'initial damage threshold' given for the parameter $W\ (\equiv (W/\beta^n)\,|_{\beta=1})$.

*3.2.2. Case $c \neq 0$: rate-dependent damage evolution (visco-damage)*

For $c \neq 0$, the Legendre transform (17) leads to:

$$\Phi^*(B^{\mathrm{d}}) = \sup_{\dot{\beta}\leqslant 0}\Big\{ -\tfrac{1}{2}c\dot{\beta}^2 - g\dot{\beta}\Big\} = \frac{1}{2}\,\frac{(\langle g\rangle^+)^2}{c}, \tag{24}$$

where we have used the notation in Eq. (19) for the yield function $g$. The damage evolution in second term of Eq. (15) gives then:

$$\dot{\beta} = \frac{\partial\Phi^*(B^{\mathrm{d}})}{\partial B^{\mathrm{d}}} = \frac{\partial\Phi^*(B)}{\partial B} = -\frac{\langle g\rangle^+}{c}, \tag{25}$$

which constitutes a *Perzyna* type model of evolution. Like for visco-plasticity Simo (1988) and Simo and Hughes (1998), the constitutive relation governing visco-damage behaviour is obtained from its inviscid counterpart, Eq. (20), simply by replacing $\dot{\delta}$ by $\langle g\rangle^+/c$, $c$ being then a viscosity coefficient as originally defined in Eq. (11).

**Remark 4.** The developments of this section motivate the coupling of the actual damage formulation with plasticity. In fact, it was shown that the notion of yield criterion and flow rule are recovered for damage in the same format as for classical plasticity.

*3.3. One dimensional bifurcation analysis*

In this section we investigate the occurrence of bifurcation in an infinite one dimensional body from a homogeneous state of (positive) deformation and damage $(\epsilon_0, \beta_0)$ with the *rate-independent* damage model. The analysis derived here follows identical lines as in Pijaudier-Cabot and Burlion (1996). Besides on the expected role played by the factor of influence of damage $k$, we will also clear the role of the exponent parameter $n > 0$ defined in Eq. (11).

In statics, infinitesimal perturbation around equilibrium where (positive) strain and damage are initially homogeneous have to satisfy the following coupled equations:

$$\dot{\sigma}_{,x} = 0, \qquad -k\dot{\beta}_{,xx} + \overline{\dot{\beta^n S(\epsilon)}} = 0, \tag{26}$$

where $(\ )_{,x}$ stands for the derivative with respect to $x$ and where we have taken $c = 0$ (rate-independent). In our one dimensional problem, the stress–strain relation is given by $\sigma = \beta E\epsilon$ and expression (12) leads to $S(\epsilon) = \frac{1}{2}E\epsilon^2$ ($\epsilon$ is positive), where $E$ is the Young's modulus. Taking the rate forms of these expressions and replacing them into Eq. (26) gives:

$$\beta_0 E\dot{\epsilon}_{,x} + E\epsilon_0\dot{\beta}_{,x} = 0, \tag{27}$$

$$-k\dot{\beta}_{,xx} + nS(\epsilon_0)\beta_0^{(n-1)}\dot{\beta} + \beta_0^n S'(\epsilon_0)\dot{\epsilon} = 0, \tag{28}$$

where $S'(\epsilon_0) = E\epsilon_0$. When Eq. (28) is derived with respect to $x$, $\dot{\epsilon}_{,x}$ is obtained as a function of $\dot{\beta}_{,x}$ and $\dot{\beta}_{,xxx}$. Substitution of this result along with the expressions of $S(\epsilon_0)$ and $S'(\epsilon_0)$ into Eq. (27) yields:

$$\frac{2k}{E(2-n)\beta_0^{(n-1)}\epsilon_0^2}\dot{\beta}_{,xxx} + \dot{\beta}_{,x} = 0. \tag{29}$$

The wavelengths $l$ of the solutions are then function of the initial homogeneous state $(\epsilon_0, \beta_0)$ and the material parameters $k$ and $n$:

$$l = 2\Pi \sqrt{\frac{2k}{E\epsilon_0^2}} \sqrt{\frac{\beta_0^{(1-n)}}{2-n}}. \tag{30}$$

A well known result of bifurcation analysis states that softening is encountered when the term under the square root sign in Eq. (30) is positive. Inspection of this expression leads then to the following noteworthy conclusions. As the term $2k/E\epsilon_0^2$ is always positive if $k \neq 0$, we arrive at the following results:

(1) if $n < 2$, $l$ is real: then softening occurs.
(2) if $n > 2$, $l$ is imaginary: no softening occurs (hardening).
(3) the case $n = 2$ is the exact limit between softening and hardening.

These results show the role exhibited by the exponent parameter $n$ given in Eq. (11). Also, and as expected, harmonic solutions are found upon softening only. The wavelengths of the solutions are then function of the initial state and are controlled by the factor of influence of damage $k$.

## 4. Formulation of the elastoplastic-damage modelling

In this section, the damage formalism outlined in the last sections is combined with plasticity. A theoretical framework for elastoplastic-damage modelling is given followed by an example of application. Noteworthy remarks are given throughout this section.

### 4.1. Theoretical framework

#### 4.1.1. Thermodynamical basis

As in classical infinitesimal plasticity, we consider the additive decomposition of the total infinitesimal strain tensor $\boldsymbol{\epsilon}$ into an elastic part $\boldsymbol{\epsilon}^{\mathrm{e}}$ and a plastic part $\boldsymbol{\epsilon}^{\mathrm{p}}$, $\boldsymbol{\epsilon} = \boldsymbol{\epsilon}^{\mathrm{e}} + \boldsymbol{\epsilon}^{\mathrm{p}}$.

Within the framework of continuum thermodynamics, and following the developments given in Section 2.2, the free energy $\Psi$ has now the form

$$\Psi \equiv \Psi(\boldsymbol{\epsilon}^{\mathrm{e}} = \boldsymbol{\epsilon} - \boldsymbol{\epsilon}^{\mathrm{p}}, \beta, \operatorname{grad}\beta, \boldsymbol{\xi}), \tag{31}$$

where $\boldsymbol{\xi}$ is a suitable vector of internal (strain-like) plastic variables. We assume again that the internal work of damage $B$ is additively decomposed into a reversible part, $B^{\mathrm{r}}$, and a dissipative part, $B^{\mathrm{d}}$, $B = B^{\mathrm{r}} + B^{\mathrm{d}}$. By taking the time derivative of $\Psi$ in Eq. (31), substituting into the Clausius–Duhem inequality (5) and making use of standard arguments Coleman and Noll (1963) and Coleman and Gurtin (1967), one obtains:

$$\boldsymbol{\sigma} = \frac{\partial\Psi}{\partial\boldsymbol{\epsilon}^{\mathrm{e}}} = \frac{\partial\Psi}{\partial\boldsymbol{\epsilon}}, \qquad \mathbf{H} = \frac{\partial\Psi}{\partial(\operatorname{grad}\beta)}, \qquad B^{\mathrm{r}} = \frac{\partial\Psi}{\partial\beta}, \qquad \mathbf{q} = -\frac{\partial\Psi}{\partial\boldsymbol{\xi}}, \tag{32}$$

together with the dissipative inequality

$$\boldsymbol{\sigma} : \dot{\boldsymbol{\epsilon}}^{\mathrm{p}} + \mathbf{q} \cdot \dot{\boldsymbol{\xi}} + B^{\mathrm{d}}\dot{\beta} \geqslant 0, \tag{33}$$

where $\mathbf{q}$ denotes the vector of internal (stress-like) plastic variables conjugate to $\boldsymbol{\xi}$.

As in Section 2.2, we postulate the existence of a pseudo-potential of dissipation $\Phi$, now of the form

$$\Phi \equiv \Phi(\dot{\beta}, \dot{\boldsymbol{\epsilon}}^{\mathrm{p}}, \dot{\boldsymbol{\xi}}; \boldsymbol{\epsilon}, \boldsymbol{\epsilon}^{\mathrm{p}}, \beta, \boldsymbol{\xi}), \tag{34}$$

where the state variables $\boldsymbol{\epsilon}$, $\boldsymbol{\epsilon}^{\mathrm{p}}$, $\beta$ and $\boldsymbol{\xi}$ have the *possibility* to act as parameters. This function is positive, convex and sub-differentiable with $\Phi(\dot{\beta}, \dot{\boldsymbol{\epsilon}}^{\mathrm{p}}, \dot{\boldsymbol{\xi}}) = 0$ for $(\dot{\beta}, \dot{\boldsymbol{\epsilon}}^{\mathrm{p}}, \dot{\boldsymbol{\xi}}) = (0, \mathbf{0}, \mathbf{0})$. Thus, the following complementary laws

$$\boldsymbol{\sigma} = \frac{\partial \Phi}{\partial \dot{\boldsymbol{\epsilon}}^{\mathrm{p}}}, \qquad \mathbf{q} = \frac{\partial \Phi}{\partial \dot{\boldsymbol{\xi}}}, \qquad B^{\mathrm{d}} = \frac{\partial \Phi}{\partial \dot{\beta}}, \tag{35}$$

are sufficient to satisfy the inequality (33) for any admissible process.

From the practical standpoint, the laws of plasticity (coupled with damage) (35) (first and second terms) are not suitable. Classically, it is more convenient to express them in a form of evolution laws of the flux variables $(\dot{\boldsymbol{\epsilon}}^{\mathrm{p}}, \dot{\boldsymbol{\xi}})$ function of the dual variables $(\boldsymbol{\sigma}, \mathbf{q})$. This is accomplished with the *Legendre* transform of the pseudo-potential of dissipation $\Phi$ as shown below.

*4.1.2. Characterization of plastic response*

We first consider a free energy of the following form:

$$\Psi(\boldsymbol{\epsilon} - \boldsymbol{\epsilon}^{\mathrm{p}}, \beta, \operatorname{grad}\beta, \boldsymbol{\xi}) = \Psi^{\mathrm{ed}}(\boldsymbol{\epsilon} - \boldsymbol{\epsilon}^{\mathrm{p}}, \beta, \operatorname{grad}\beta) + \Psi^{\mathrm{p}}(\boldsymbol{\xi}), \tag{36}$$

where $\Psi^{\mathrm{ed}}$ is the elastic-damage part of the free energy of the type given by Eq. (10), i.e. where $\boldsymbol{\epsilon}$ is replaced by $\boldsymbol{\epsilon} - \boldsymbol{\epsilon}^{\mathrm{p}} = \boldsymbol{\epsilon}^{\mathrm{e}}$, and $\Psi^{\mathrm{p}}$ denotes a general plastic potential function. For example, to define a linear isotropic plastic hardening mechanism, the vector of internal strain-like plastic variables $\boldsymbol{\xi}$ is replaced by the (scalar) equivalent plastic strain $e^{\mathrm{p}} \geqslant 0$ and $\Psi^{\mathrm{p}}$ is then given by a quadratic hardening potential with expression $\Psi^{\mathrm{p}}(e^{\mathrm{p}}) = \frac{1}{2} h e^{\mathrm{p}^2}$, where $h > 0$ is the plastic modulus.

Thus, the constitutive laws (32) (first and fourth terms) are expressed as:

$$\boldsymbol{\sigma} = \frac{\partial \Psi^{\mathrm{ed}}}{\partial \boldsymbol{\epsilon}}(\boldsymbol{\epsilon} - \boldsymbol{\epsilon}^{\mathrm{p}}, \beta, \operatorname{grad}\beta), \qquad \mathbf{q} = -\frac{\partial \Psi^{\mathrm{p}}}{\partial \boldsymbol{\xi}}(\boldsymbol{\xi}). \tag{37}$$

It remains now to give a general expression of the pseudo-potential of dissipation $\Phi$. The key idea is to split it into two parts as follows:

$$\Phi(\dot{\beta}, \dot{\boldsymbol{\epsilon}}^{\mathrm{p}}, \dot{\boldsymbol{\xi}}; \boldsymbol{\epsilon}, \boldsymbol{\epsilon}^{\mathrm{p}}, \beta, \boldsymbol{\xi}) = \Phi^{\mathrm{p}}(\dot{\boldsymbol{\epsilon}}^{\mathrm{p}}, \dot{\boldsymbol{\xi}}; \beta, \boldsymbol{\xi}) + \Phi^{\mathrm{d}}(\dot{\beta}; \boldsymbol{\epsilon}, \boldsymbol{\epsilon}^{\mathrm{p}}, \beta, \boldsymbol{\xi}). \tag{38}$$

$\Phi^{\mathrm{d}}$ is the damage part of the dissipative function of the type given by Eq. (11), and $\Phi^{\mathrm{p}}$ is its plastic part. Note that $\Phi^{\mathrm{p}}(\dot{\boldsymbol{\epsilon}}^{\mathrm{p}}, \dot{\boldsymbol{\xi}})$ must be positively homogeneous of degree one for rate-independent plasticity.

Furthermore, for rate-independent plasticity, $\Phi^{\mathrm{p}}$ is such that its Legendre transform

$$\Phi^{\mathrm{p}^*}(\boldsymbol{\sigma}, \mathbf{q}; \beta, \boldsymbol{\xi}) = \sup_{\dot{\boldsymbol{\epsilon}}^{\mathrm{p}}, \dot{\boldsymbol{\xi}}} \{\boldsymbol{\sigma} : \dot{\boldsymbol{\epsilon}}^{\mathrm{p}} + \mathbf{q} \cdot \dot{\boldsymbol{\xi}} - \Phi^{\mathrm{p}}(\dot{\boldsymbol{\epsilon}}^{\mathrm{p}}, \dot{\boldsymbol{\xi}}; \beta, \boldsymbol{\xi})\}, \tag{39}$$

leads to the following result

$$\Phi^{\mathrm{p}^*}(\boldsymbol{\sigma}, \mathbf{q}; \beta, \boldsymbol{\xi}) = I_{\{f(\boldsymbol{\sigma}, \mathbf{q}; \beta, \boldsymbol{\xi}) \leqslant 0\}}, \tag{40}$$

where $f(\boldsymbol{\sigma}, \mathbf{q})$ is a convex function. From a physical standpoint, $f(\boldsymbol{\sigma}, \mathbf{q})$ constitutes a (single-surface) yield criterion characterizing the elastic-damage domain as in classical elastoplasticity coupled to damage, see Lemaitre (1992) and Simo and Ju (1987a,b) among others. Then, for the simplest assumption of *associative* plasticity, the evolution equations for the internal flux variables $(\dot{\boldsymbol{\epsilon}}^{\mathrm{p}}, \dot{\boldsymbol{\xi}})$ are given by the standard relations:

$$\dot{\boldsymbol{\epsilon}}^{\mathrm{p}} = \frac{\partial \Phi^*}{\partial \boldsymbol{\sigma}} = \frac{\partial \Phi^{\mathrm{p}^*}}{\partial \boldsymbol{\sigma}} = \dot{\gamma} \frac{\partial f}{\partial \boldsymbol{\sigma}}, \tag{41}$$

$$\dot{\boldsymbol{\xi}} = \frac{\partial \Phi^*}{\partial \mathbf{q}} = \frac{\partial \Phi^{\mathrm{p}^*}}{\partial \mathbf{q}} = \dot{\gamma}\frac{\partial f}{\partial \mathbf{q}}, \tag{42}$$

together with the Kuhn–Tucker *loading/unloading* conditions:

$$\dot{\gamma} \geqslant 0, \quad f(\boldsymbol{\sigma}, \mathbf{q}; \beta, \boldsymbol{\xi}) \leqslant 0, \quad \dot{\gamma} f(\boldsymbol{\sigma}, \mathbf{q}; \beta, \boldsymbol{\xi}) = 0, \tag{43}$$

where $\dot{\gamma}$ is the plastic consistency parameter and $\Phi^*$ is the *total* Legendre transform of $\Phi$.

**Remark 5.** The choice of an additive split of the pseudo-potential of dissipation $\Phi$ in (38) permits to obtain the standard format of the classical plastic models (41)–(43).

**Remark 6.** Viscoplasticity (rate-dependent) can also be recovered by choosing $\Phi^{\mathrm{p}}$ as a convex function not positively homogeneous of degree one. As for visco-damage (Section 3.2), Perzyna type models can also be obtained from their inviscid counterpart, see for example Simo and Hughes (1998) among others.

*4.1.3. Characterization of damage*

Following the choices made for the general forms of the free energy $\Psi$ in Eq. (36) and the dissipation function $\Phi$ in Eq. (38), the formulation of damage evolution can either be characterized by the formalism given in Section 3.1 or by its alternative counterpart given in Section 3.2.

From the second term of Eq. (32) and Eq. (36), one has

$$\mathbf{H} = \frac{\partial \Psi^{\mathrm{ed}}}{\partial(\operatorname{grad}\beta)}, \tag{44}$$

and from the third term of Eqs. (32) and (35) and from Eqs. (36) and (38), one has for the internal work of damage

$$B = \frac{\partial \Psi^{\mathrm{ed}}}{\partial \beta} + \frac{\partial \Phi^{\mathrm{d}}}{\partial \dot{\beta}}. \tag{45}$$

Following the developments of Section 3.2, Eq. (45) can alternatively be transformed in an evolution law of the damage rate $\dot{\beta}$ function of the internal work of damage

$$\dot{\beta} = \frac{\partial \Phi^{\mathrm{d}^*}}{\partial B^{\mathrm{d}}}(B^{\mathrm{d}}), \tag{46}$$

where $\Phi^{\mathrm{d}^*}(B^{\mathrm{d}})$ is the Legendre transform of $\Phi^{\mathrm{d}}(\dot{\beta})$.

*4.2. An example of elastoplastic-damage model*

As an example of application of the preceding framework, we give in this subsection a simple elasto-plastic-damage model. For the damage part, we use the rate-independent version of the model outlined in Section 3, i.e with $c = 0$, while for the plastic part, we use the classical $J_2$-flow theory with *perfect* plasticity coupled with damage.

The free energy in Eq. (36) is given by

$$\Psi \equiv \Psi^{\mathrm{ed}} = \tfrac{1}{2}\beta(\boldsymbol{\epsilon} - \boldsymbol{\epsilon}^{\mathrm{p}}) : \mathbf{C} : (\boldsymbol{\epsilon} - \boldsymbol{\epsilon}^{\mathrm{p}}) + \tfrac{1}{2}k(\operatorname{grad}\beta)^2, \tag{47}$$

since $\boldsymbol{\xi} \equiv \mathbf{0}$ and $\Psi^{\mathrm{p}} \equiv 0$ for perfect plasticity.

Although the choice of the plastic part $\Phi^{\mathrm{p}}$ of $\Phi$ in Eq. (38) is not an obvious task in general (see Remark 7 below), for the present plastic flow under consideration, however, it has a simple well-known expression Germain (1973). The choices of the two parts $\Phi^{\mathrm{p}}$ and $\Phi^{\mathrm{d}}$ of $\Phi$ in Eq. (38) are given by

$$\Phi^{\mathrm{p}}(\dot{\boldsymbol{\epsilon}}^{\mathrm{p}};\ \beta) = \beta\sqrt{\frac{2}{3}}\,\sigma_y\|\dot{\boldsymbol{\epsilon}}^{\mathrm{p}}\|, \tag{48}$$

$$\Phi^{\mathrm{ed}} = -\dot{\beta}\big\{W + \tfrac{1}{2}(\boldsymbol{\epsilon}-\boldsymbol{\epsilon}^{\mathrm{p}}) : \mathbf{C} : (\boldsymbol{\epsilon}-\boldsymbol{\epsilon}^{\mathrm{p}}) - \beta^n S(\boldsymbol{\epsilon})\big\} + I_-(\dot{\beta}), \tag{49}$$

where the norm $\|\cdot\|$ is defined by $\|\cdot\| = [(\cdot):(\cdot)]^{1/2}$ and where we have used the definition (12) for $S(\boldsymbol{\epsilon})$. Here the total strain tensor $\boldsymbol{\epsilon}$ is used to define $S(\boldsymbol{\epsilon})$. Of course other choices are also possible as shown in the example of Section 6.6. $\sigma_y$ is the flow stress as it will be shown below. $\Phi^{\mathrm{p}}$ and $\Phi^{\mathrm{ed}}$ are clearly positively homogeneous functions of degree one.

Since $\mathrm{tr}[\boldsymbol{\epsilon}^{\mathrm{p}}] = 0$, the Legendre transform $\Phi^{\mathrm{p}^*}$ (Eq. (39)) of $\Phi^{\mathrm{p}}$, or in other words, the partial Legendre transform of $\Phi$ in Eq. (38) with respect to $\dot{\boldsymbol{\epsilon}}^{\mathrm{p}}$, results in the indicator function of the following yield criterion (Eq. (40)):

$$f(\boldsymbol{\sigma};\ \beta) = \frac{\|\mathrm{dev}[\boldsymbol{\sigma}]\|}{\beta} - \sqrt{\frac{2}{3}}\,\sigma_y \leqslant 0, \tag{50}$$

where dev denotes the deviator operator. The criterion (50) is then the well known yield function of $J_2$-flow perfect plasticity formulated in terms of the effective stress $\boldsymbol{\sigma}/\beta$, see Lemaitre and Chaboche (1988), Lemaitre (1992) and Simo and Ju (1987a,b) among others.

Total Legendre transform of $\Phi = \Phi^{\mathrm{p}} + \Phi^{\mathrm{d}}$ gives, besides on the yield criterion (50) relative to plasticity, also the yield criterion (21) relative to damage.

Substitution of Eqs. (47) and (49) into first term of Eq. (37) and Eqs. (44) and (45) gives the constitutive relations

$$\boldsymbol{\sigma} = \beta\mathbf{C} : (\boldsymbol{\epsilon}-\boldsymbol{\epsilon}^{\mathrm{p}}), \qquad \mathbf{H} = k\,\mathrm{grad}\,\beta, \qquad B \in \beta^n S(\boldsymbol{\epsilon}) + \partial I_-(\dot{\beta}). \tag{51}$$

By replacing the last results into Eqs. (3) and (4) in statics, we obtain the following equations of motion:

$$\begin{aligned} \mathrm{div}(\beta\mathbf{C} : (\boldsymbol{\epsilon}-\boldsymbol{\epsilon}^{\mathrm{p}})) + \mathbf{f} = \mathbf{0} \quad &\text{in } \Omega, \\ \boldsymbol{\sigma}\cdot\mathbf{n} = \mathbf{F} \quad &\text{on } \partial\Omega, \end{aligned} \tag{52}$$

$$\begin{aligned} -k\Delta\beta + \beta^n S(\boldsymbol{\epsilon}) + \partial I_-(\dot{\beta}) \ni W \quad &\text{in } \Omega, \\ k\tfrac{\partial\beta}{\partial\mathbf{n}} = 0 \quad &\text{on } \partial\Omega, \end{aligned} \tag{53}$$

which have to be solved together with the (*local*) evolution equation for the plasticity

$$\dot{\boldsymbol{\epsilon}}^{\mathrm{p}} = \dot{\gamma}\frac{\partial f}{\partial\boldsymbol{\sigma}}(\boldsymbol{\sigma};\beta), \tag{54}$$

$$\dot{\gamma} \geqslant 0, \quad f(\boldsymbol{\sigma};\beta) \leqslant 0, \quad \dot{\gamma} f(\boldsymbol{\sigma};\beta) = 0. \tag{55}$$

**Remark 7.** As the choice of the plastic part of the pseudo-potential of dissipation is not obvious, for all the future developments there is no need to give explicit expressions for $\Phi^{\mathrm{p}}$ as in Eq. (48). The plastic part of the modelling will be given directly in standard format by means of a (convex) yield criterion, which is physically meaningful, together with the plastic flow rules. In fact, and as it was shown in the last example, the standard format is compatible with the framework outlined in this section.

**Remark 8.** From the theoretical and numerical points of view, the damage part of the modelling can be treated indifferently from the formalism given in Section 3.1 or by its alternative form given in Section 3.2.

## 5. Variational formulation and resolution algorithm

The variational formulation of the local form of the governing equations plays a central role in the numerical solution of the boundary value problem. In this section, we first develop the variational framework which constitutes the basis of our subsequent algorithmic treatment. Without loss of generality, in the developments that follow we shall neglect inertia effects and confine our attention to the static problem.

### 5.1. Variational framework

In statics, the two governing equations of motion (3) and (4) are equivalent to the two following weak forms:

$$R(\mathbf{u},\beta,\boldsymbol{\eta}) \equiv \int_{\Omega} \boldsymbol{\sigma}(\mathbf{u},\beta,\boldsymbol{\epsilon}^{\mathrm{p}},\boldsymbol{\xi}) : \nabla^{\mathrm{s}}\boldsymbol{\eta}\,\mathrm{d}\Omega - \int_{\Omega} \mathbf{f}\cdot\boldsymbol{\eta}\,\mathrm{d}\Omega - \int_{\partial\Omega} \mathbf{F}\cdot\boldsymbol{\eta}\,\mathrm{d}\Gamma = 0, \tag{56}$$

$$\int_{\Omega} \operatorname{div}\mathbf{H}\psi\,\mathrm{d}\Omega - \int_{\Omega} B\psi\,\mathrm{d}\Omega = 0, \tag{57}$$

for any admissible variations of displacement and damage, $\boldsymbol{\eta}$ and $\psi$, respectively, and where $\mathbf{u}$ is here the displacement field.

The coupled variational boundary value problems (56) and (57) is to be solved incrementally with the following *local* rate constitutive equations for general plasticity appended (see Remark 7):

$$\begin{cases} \dot{\boldsymbol{\epsilon}} = \nabla^{\mathrm{s}}\dot{\mathbf{u}}, \\ \dot{\boldsymbol{\epsilon}}^{\mathrm{p}} = \dot{\gamma}\boldsymbol{\nu}(\boldsymbol{\sigma},\mathbf{q};\beta), \\ \dot{\boldsymbol{\xi}} = \dot{\gamma}\mathbf{h}(\boldsymbol{\sigma},\mathbf{q};\beta), \end{cases} \\ \dot{\gamma} \geqslant 0, \quad f(\boldsymbol{\sigma},\mathbf{q};\beta) \leqslant 0, \quad \dot{\gamma} f(\boldsymbol{\sigma},\mathbf{q};\beta) = 0, \tag{58}$$

where second term of Eq. (58) expresses a generally non-associated flow rule for the plastic strain rates ($\boldsymbol{\nu}$ being the plastic flow direction) and the third term of Eq. (58) represents some suitable set of hardening laws governing the evolution of the internal plastic variables ($\mathbf{h}$ being the plastic moduli). For the particular case of associated plasticity (see Eqs. (41) and (42)), one has $\boldsymbol{\nu} = \partial f/\partial\boldsymbol{\sigma}$ and $\mathbf{h} = \partial f/\partial\mathbf{q}$.

In Eqs. (56) and (57), $\boldsymbol{\sigma}$, $\mathbf{H}$ and $B$ follow from the constitutive relations first term of Eq. (37), Eqs. (44) and (45). From the above developments, the simplest expressions for $\boldsymbol{\sigma}$ and $\mathbf{H}$ are given by: $\boldsymbol{\sigma} = \beta\mathbf{C} : (\boldsymbol{\epsilon} - \boldsymbol{\epsilon}^{\mathrm{p}})$ and $\mathbf{H} = k\operatorname{grad}\beta$ (see the first and second terms of Eq. (51)), while the internal work of damage $B$ depends on both $\Psi^{\mathrm{ed}}$ and $\Phi^{\mathrm{d}}$ (see Eq. (45)).

For the sake of clarity, we prefer to continue our developments by particularizing the damage part of the model. For this, and without loss of generality, we choose the *rate-independent* version of the model outlined in Section 3 (see also its use in the example of Section 4.2). Note that the rate-dependent case (visco-damage) is obtained simply by adding the term corresponding to $c\dot{\beta}$ (see first term of Eq. (14)) in the damage evolution equation and then by performing a time-stepping scheme (typically the implicit backward-Euler scheme).

Let us note that the (*non-smooth*) indicator function $I_{-}(\dot{\beta})$ (in Eq. (49) or in Eq. (11) leads to the presence of the generalized derivative $\partial I_{-}(\dot{\beta})$ in the damage part of the equations of motion (Eq. (53) or Eq. (14)). This generalized derivative constitutes in fact a *mathematical* reaction which forces the physically meaningful constraint $\dot{\beta} \leqslant 0$. If $I_{-}(\dot{\beta})$ is approximated by a *smooth* function, then $\partial I_{-}(\dot{\beta})$ is approximated by a classical derivative. However, in what follows this approximation will not be done and its representation will be forced by imposing the constraint $\dot{\beta} \leqslant 0$ at the outset. This particular point is still an open question actually under investigation.

Then, replacing $B$ and $\mathbf{H}$ by their respective expressions, use of the divergence theorem and taking into account the boundary condition (53) (second term) or (14)) which follow from second term of Eq. (4), Eq. (57) leads to:

$$r(\beta,\mathbf{u},\psi)\equiv\int_\Omega k\,\mathrm{grad}\,\beta\cdot\mathrm{grad}\,\psi\,\mathrm{d}\Omega+\int_\Omega S(\boldsymbol{\epsilon})\beta^n\psi\,\mathrm{d}\Omega-\int_\Omega W\psi\,\mathrm{d}\Omega=0,\quad\dot\beta\leqslant 0. \tag{59}$$

The elastoplastic-damage problem to be solved is then given by the coupled weak forms (56) and (59) together with the local evolution Eq. (58).

### 5.2. Linearization and resolution algorithm

Within the context of the finite element method, the solution of the coupled problem (56), (58) and (59) is chosen to be accomplished as follows. During the resolution algorithm, the two field Eqs. (56) and (59) are *decoupled*. Eq. (56) is solved at fixed damage to determine the displacement field, and Eq. (59) is solved at fixed displacement (strain) to determine the damage field. Accordingly, the numerical solution of the nonlinear problem is based on an *iterative* solution procedure of a discretized version of the weak forms (56) and (59). Typically, the following steps are involved:

*Step 1*. The discretized equation (56) at fixed damage generates incremental motions $\Delta\mathbf{u}$ which, in turn, are used to calculate the incremental strain history by means of the kinematic relations.
*Step 2*. For a given incremental strain, new values of the state variables $\{\boldsymbol{\sigma},\boldsymbol{\epsilon}^{\mathrm{p}},\boldsymbol{\xi}\}$ are obtained (for fixed damage) by integration of the *local* constitutive equations (58) with given initial conditions.
*Step 3*. For fixed displacement and plasticity $\{\boldsymbol{\epsilon},\boldsymbol{\epsilon}^{\mathrm{p}},\boldsymbol{\xi}\}_{\mathrm{fixed}}$, the discretized equation (59) generates incremental damage $\Delta\beta$ (with $\dot\beta\leqslant 0$ forced).
*Step 4*. The discrete equation (56) is tested for the computed stresses and, if violated, the iteration process is continued by returning to Step 1.

*Steps 1*, *3* and *4* are carried out at a global level by the finite element procedure. Steps **1** and **3** require the linearized variational forms of Eqs. (56) and (59), respectively. From a specified initial data at time $t=t_n$, the linearization of the weak form (56) (Step **1**) is given by:

$$DR(\mathbf{u}^i_{n+1},\beta^i_{n+1},\boldsymbol{\eta})\cdot\Delta\mathbf{u}^i_{n+1}\equiv\int_\Omega\nabla^{\mathrm{s}}\boldsymbol{\eta}:[\mathbf{C}^i_{n+1}:\nabla^{\mathrm{s}}(\Delta\mathbf{u}^i_{n+1})]\,\mathrm{d}\Omega=-R(\mathbf{u}^i_{n+1},\beta^i_{n+1},\boldsymbol{\eta}), \tag{60}$$

and the linearization of the weak form (59) (Step **3**) is given by:

$$\begin{aligned}Dr(\beta^i_{n+1},\mathbf{u}^i_{n+1},\psi)\Delta\beta^i_{n+1}&\equiv\int_\Omega k\,\mathrm{grad}\,\psi\cdot\mathrm{grad}\,\Delta\beta^i_{n+1}\,\mathrm{d}\Omega+\int_\Omega\psi S(\boldsymbol{\epsilon}^i_{n+1})n(\beta^i_{n+1})^{n-1}\Delta\beta^i_{n+1}\,\mathrm{d}\Omega\\&=-r(\beta^i_{n+1},\mathbf{u}^i_{n+1},\psi),\quad\dot\beta\leqslant 0.\end{aligned} \tag{61}$$

Accordingly, one solves a sequence of successive linearized problems, (60) and (61), until the residuals $R(\mathbf{u}^i_{n+1},\beta^i_{n+1},\boldsymbol{\eta})$ and $r(\beta^i_{n+1},\mathbf{u}^i_{n+1},\psi)$ vanish to within a prescribed tolerance. In Eqs. (60) and (61), subscripts refer to the time step and the superscripts to the iteration within the time step. In Eq. (60), $\mathbf{C}^i_{n+1}$ are the elastoplastic-damage tangent moduli at fixed damage.

**Remark 9.** The decoupling during the resolution algorithm is due to the fact that Eqs. (60) and (61) cannot be coupled as for classical coupled problems, i.e. by means of a monolithic scheme. This is because of the choice made for the algorithmic treatment of the physical constraint $\dot\beta\leqslant 0$ present in Eq. (61). Clearly this treatment differs from the one used for local damage models. In fact, if the gradient of damage variable

were not introduced in the formulation, i.e. for $k = 0$, the damage part of the problem would then be solved locally in a classical manner with the history variable $r(t) = (W/\beta^n(t))$, $\dot{r}(t) \geqslant 0$ (see Remark 3). Of course, this is not the goal of this study.

**Remark 10.** Because of the decoupled algorithmic treatment, the expression of the tangent moduli $\mathbf{C}^i_{n+1}$ in Eq. (60) is given simply by the classical elastoplastic tangent moduli multiplied by the value $\beta^i_{n+1}$ of the damage state variable at iteration $i$.

The Eq. (60), which follows from Eq. (56), is a function of the stresses $\boldsymbol{\sigma}$ (evaluated at the Gauss points) which in turn, are defined in terms of strain and damage history by the *local* problem of evolution (58). Thus, the sequence of linearized problems (60) are obtained by numerically integrating problem (58) (Step 2). This is discussed in the Section 5.3.

### 5.3. The local problem of evolution. Integration algorithm for plasticity

In this section we are concerned with Step 2 of the resolution algorithm. From an algorithmic point of view, the problem of integrating the constrained evolution Eq. (58) is performed *locally* at each Gauss point of a typical finite element. Accordingly, as damage is considered as a fixed parameter in this step, the integration procedure follows *exactly* the same lines as in classical elastoplasticity, see Ortiz and Simo (1986), Simo and Hughes (1987, 1998), Simo and Ju (1987a,b) and Simo and Taylor (1985) among others.

Using the notion of *operator split*, we consider the following decomposition of the evolution Eq. (58) into an elastic-damage and plastic parts:

- *Problem 1*: Trial elastic-damage state (elastic-damage predictor)

$$\left\{\begin{array}{l} \dot{\boldsymbol{\epsilon}} = \nabla^{\mathrm{s}}\dot{\mathbf{u}}, \\ \dot{\boldsymbol{\epsilon}}^{\mathrm{p}} = \mathbf{0}, \\ \dot{\boldsymbol{\xi}} = \mathbf{0}, \end{array}\right. \qquad \text{constraint : none.} \tag{62}$$

- *Problem 2*: Return mapping (plastic corrector)

$$\left\{\begin{array}{l} \dot{\boldsymbol{\epsilon}} = \mathbf{0}, \\ \dot{\boldsymbol{\epsilon}}^{\mathrm{p}} = \dot{\gamma}\boldsymbol{\nu}(\boldsymbol{\sigma}, \mathbf{q}; \beta^i_{n+1}), \\ \dot{\boldsymbol{\xi}} = \dot{\gamma}\mathbf{h}(\boldsymbol{\sigma}, \mathbf{q}; \beta^i_{n+1}), \end{array}\right. \qquad \text{constraint : } \dot{\gamma} \geqslant 0, \quad f(\boldsymbol{\sigma}, \mathbf{q}; \beta^i_{n+1}) \leqslant 0, \quad \dot{\gamma} f(\boldsymbol{\sigma}, \mathbf{q}; \beta^i_{n+1}) = 0. \tag{63}$$

One can check that Eqs. (62) and (63) do indeed add up to Eq. (58) in agreement with the notion of operator split Ortiz and Simo (1986), Simo and Hughes (1987, 1998) and Simo and Ju (1987a,b).

#### 5.3.1. Problem 1: The trial elastic-damage state

This problem is obtained from the original one Eq. (58) by *freezing* the plastic flow and taking an elastic-damage step which ignores the constraint placed on the stress field by the plastic yield criterion. The trial stress tensor is obtained by mere function evaluation, while the plastic strains and the plastic internal variables remain identically equal to their respective initial values.

The solution of this problem is given by the predictor state: $\boldsymbol{\sigma}^{\mathrm{trial}}_{n+1}$ and $\mathbf{q}^{\mathrm{trial}}_{n+1} = \mathbf{q}_n$.

#### 5.3.2. Problem 2: Return mapping

In this problem, one first checks the Kuhn–Tucker loading/unloading conditions simply by evaluating the plastic criterion $f^{\mathrm{trial}}_{n+1} \equiv f(\boldsymbol{\sigma}^{\mathrm{trial}}_{n+1}, \mathbf{q}^{\mathrm{trial}}_{n+1}; \beta^i_{n+1})$. Two situations can occur:

- if $f_{n+1}^{\text{trial}} \leqslant 0$ then the elastic-damage predictor is the final state.
- else if $f_{n+1}^{\text{trial}} > 0$ then an incrementally plastic process is taking place and a plastic return mapping has to be performed.

Within the plastic return mapping corrector, the predictor stresses and internal plastic variables are returned back to the yield surface. This procedure can be handeled by any of the existing algorithms in the literature. In our case, and depending on the plastic flow model at hand, the algorithms we use for this procedure are the well known closest-point projection method which can be performed together with the use of the so-called consistent tangent operator Simo and Hughes (1987, 1998) and Simo and Taylor (1985), or the cutting-plane method Ortiz and Simo (1986) and Simo and Hughes (1987, 1998).

### 5.4. Finite element approximations and solution procedure

Due to the nature of the governing equations at hand, the damage is treated as a continuous field like for the displacements. Accordingly, within the finite element method, the same shape functions are used to interpolate the displacements and damage variables.

Let $\Omega = \bigcup_{e=1}^{n_{\text{el}}} \Omega_{\text{e}}$ be a finite element approximation constructed by means of standard *isoparametric* elements. Using *vector notation* and standard conventions in finite element analysis, see Hughes (1987) and Zienkiewicz and Taylor (1989), we write:

$$\mathbf{u}_{\text{e}} = \mathbf{u}|_{\Omega_{\text{e}}} = \mathbf{N}_{\text{e}}\mathbf{d}_{\text{e}}, \qquad \nabla^{\text{s}}\mathbf{u}_{\text{e}} = \mathbf{B}_{\text{e}}\mathbf{d}_{\text{e}}, \tag{64}$$

$$\beta_{\text{e}} = \beta|_{\Omega_{\text{e}}} = \mathbf{n}_{\text{e}}\boldsymbol{q}_{\text{e}}, \qquad \operatorname{grad}\beta_{\text{e}} = \mathbf{b}_{\text{e}}\mathbf{q}_{\text{e}}, \tag{65}$$

where $\mathbf{d}_{\text{e}}$ is the vector of element nodal displacements, $\mathbf{q}_{\text{e}}$ is the vector of element nodal damage, $\mathbf{N}_{\text{e}}$ and $\mathbf{n}_{\text{e}}$ are vectors of element shape functions and, $\mathbf{B}_{\text{e}}$ and $\mathbf{b}_{\text{e}}$ are the discrete strain and gradient operators, respectively.

Substitution of the preceding interpolations into Eqs. (56) and (59) yields the discrete nonlinear equations

$$\mathbf{A}_{\text{e}=1}^{n_{\text{el}}}[\mathbf{f}_{\text{e}}^{\text{int}}(\mathbf{d}_{\text{e}};\mathbf{q}_{\text{e}}) - \mathbf{f}_{\text{e}}^{\text{ext}}] = \mathbf{0}, \tag{66}$$

$$\mathbf{A}_{\text{e}=1}^{n_{\text{el}}}[\mathbf{r}_{\text{e}}(\mathbf{q}_{\text{e}};\mathbf{d}_{\text{e}})] = \mathbf{0}, \tag{67}$$

where $\mathbf{A}$ denotes the standard assembly operator, and

$$\mathbf{f}_{\text{e}}^{\text{int}}(\mathbf{d}_{\text{e}};\mathbf{q}_{\text{e}}) = \int_{\Omega_{\text{e}}} \mathbf{B}_{\text{e}}^{\text{T}}\boldsymbol{\sigma}\,\mathrm{d}\Omega_{\text{e}}, \tag{68}$$

$$\mathbf{r}_{\text{e}}(\mathbf{q}_{\text{e}};\mathbf{d}_{\text{e}}) = \int_{\Omega_{\text{e}}} [\mathbf{b}_{\text{e}}^{\text{T}} k \operatorname{grad}\beta + \mathbf{n}_{\text{e}}^{\text{T}}\{S(\boldsymbol{\epsilon})\beta^{n} - W\}]\,\mathrm{d}\Omega_{\text{e}}. \tag{69}$$

In Eq. (66), the element external force vector $\mathbf{f}_{\text{e}}^{\text{ext}}$ has the usual expression of the standard finite element method.

Following the resolution algorithm given in Section 5.2, the solution of the elastoplastic-damage problem is performed iteratively using the following algorithm:

**a.** From an equilibrium state at time $t = t_n$, initialize displacements, damage and all the internal plastic variables: $i = 0, \quad (\cdot)_{n+1}^{0} = (\cdot)_{n}$

**b.** Compute at the element level and for each Gauss point: $\boldsymbol{\sigma}_{n+1}^{(i)}$, $\mathbf{C}_{n+1}^{(i)}$ and update internal plastic variables (at fixed damage) using a *standard return mapping* algorithm.

**c.** Integrate element matrices and residuals (Eq. (60)):

$$\mathbf{k}^{(i)}_{\mathrm{e}_{\mathrm{disp}}} = \int_{\Omega_{\mathrm{e}}} \mathbf{B}^{\mathrm{T}}_{\mathrm{e}} \mathbf{C}^{(i)}_{n+1} \mathbf{B}_{\mathrm{e}} \, \mathrm{d}\Omega_{\mathrm{e}}, \qquad \mathbf{f}^{\mathrm{int}^{(i)}}_{\mathrm{e}} = \int_{\Omega_{\mathrm{e}}} \mathbf{B}^{\mathrm{T}}_{\mathrm{e}} \boldsymbol{\sigma}^{(i)}_{n+1} \, \mathrm{d}\Omega_{\mathrm{e}},$$

**d.** Assemble and solve for a new displacement increment:

$$\mathbf{R}^{(i)} = \mathbf{A}_{e=1}^{n_{\mathrm{el}}} \left[ \mathbf{f}^{\mathrm{ext}}_{\mathrm{e}} - \mathbf{f}^{\mathrm{int}^{(i)}}_{\mathrm{e}} \right], \qquad \mathbf{K}^{(i)}_{\mathrm{disp}} = \mathbf{A}_{e=1}^{n_{\mathrm{el}}} \left[ \mathbf{k}^{(i)}_{e_{\mathrm{disp}}} \right], \qquad \Delta\mathbf{d}^{(i)} = \left[ \mathbf{K}^{(i)}_{\mathrm{disp}} \right]^{-1} \mathbf{R}^{(i)},$$

**e.** Update nodal displacements:

$$\mathbf{d}^{(i+1)} = \mathbf{d}^{(i)} + \Delta\mathbf{d}^{(i)},$$

**f.** Resolution for the damage part (at fixed displacements and internal plastic variables).

**f1**. Initialize, $\quad j = 0, \quad \mathbf{q}^{(0)}_{\mathrm{e}} = \mathbf{q}^{(i)}_{\mathrm{e}}$

**f2**. Integrate element matrices and residuals (Eq. (61)):

$$\mathbf{k}^{(j)}_{\mathrm{e}_{\mathrm{dam}}} = \int_{\Omega_{\mathrm{e}}} \left\{ \mathbf{b}^{\mathrm{T}}_{\mathrm{e}} k \mathbf{b}_{\mathrm{e}} + \mathbf{n}^{\mathrm{T}}_{\mathrm{e}} \left[ S(\boldsymbol{\epsilon}) n \beta^{(j)^{n-1}} \right] \mathbf{n}_{\mathrm{e}} \right\} \mathrm{d}\Omega_{\mathrm{e}},$$

$$\mathbf{r}^{(j)}_{\mathrm{e}} = \int_{\Omega_{\mathrm{e}}} \left\{ \mathbf{b}^{\mathrm{T}}_{\mathrm{e}} k \, \mathrm{grad}\, \beta^{(j)} + \mathbf{n}^{\mathrm{T}}_{\mathrm{e}} \left[ S(\boldsymbol{\epsilon}) \beta^{(j)^{n}} - W \right] \right\} \mathrm{d}\Omega_{\mathrm{e}},$$

**f3**. Assemble and solve for a new damage increment

$$\mathbf{r}^{(j)} = \mathbf{A}_{e=1}^{n_{\mathrm{el}}} \left[ \mathbf{r}^{(j)}_{\mathrm{e}} \right], \quad \mathbf{K}^{(j)}_{\mathrm{dam}} = \mathbf{A}_{e=1}^{n_{\mathrm{el}}} \left[ \mathbf{k}^{(j)}_{e_{\mathrm{dam}}} \right],$$

$$\Delta\mathbf{q}^{(j)} = \left[ \mathbf{K}^{(j)}_{\mathrm{dam}} \right]^{-1} \mathbf{r}^{(j)},$$

**f4**. Update nodal damage and check for convergence (of Eq. (61))

$$\mathbf{q}^{(j+1)} = \mathbf{q}^{(j)} + \Delta\mathbf{q}^{(j)},$$

**if** $\|\mathbf{r}^{(j)}\| > \mathrm{TOL1}$ **then**

set $j \leftarrow j + 1$ and GO TO **f2**

**else**

set $\mathbf{q}^{(i+1)} = \mathbf{q}^{(j+1)}$

**g.** Set $i \leftarrow i + 1$ and GO TO **b.**

Convergence of the preceding algorithm is attained when $\|\mathbf{R}^{(i)}\| < \mathrm{TOL}$.

## 6. Applications and numerical examples

As an application of the modelling framework developed in this paper, we give in this section a set of some elastoplastic-damage models together with representative numerical examples within the context of the finite element method. The first two examples are related to the elastic-damage modelling (without plasticity) to show the efficiency of the model outlined in Section 3.

Except for the example of Section 6.4, all the examples given in this section are accomplished with a rate-independent damage evolution ($c = 0$), and rate-independent plasticity (for after the next two examples).

All the models described below have been implemented in an extended version of the CESAR-LCPC finite element program Humbert (1989). The calculations were carried out using bidimensional (quadrilateral and/or triangular), plane strain, standard bilinear displacement elements (the same shape functions are used to interpolate both the displacements and the damage fields).

### 6.1. Uniaxial tension tests with the elastic-damage model

In this example, we show the stress–strain behaviours in tension predicted by the elastic-damage model outlined in Section 3. As the strain field is uniform, and hence also for the damage field, the results are not influenced by the factor of influence of damage $k$.

For fixed values of the following material parameters: $E = 35,000$ MPa (the Young's modulus), $\nu = 0.18$ (the Poisson's ratio) and the initial damage threshold $W = 6 \times 10^{-5}$ MPa, Fig. 1 shows the stress–strain behaviours in tension for different values of the exponent parameter $n$.

Note that the results of Fig. 1 meet *exactly* the conclusions of the theoretical bifurcation analysis developed in Section 3.3. That is, softening occurs for $n < 2$ while hardening occurs for $n > 2$. The case $n = 2$ is the exact limit between softening and hardening.

The role of $W$ is clear, it controls the beginning of the nonlinear phase of the behaviour.

### 6.2. Single-edge notched beam. Mesh sensitivity

This section is concerned with the numerical treatment of a single-edge notched beam subject to a three-point loading. A quite similar problem has already been treated in Peerlings et al. (1998), see also Schlangen (1993), with the difference that there, an antisymmetric four-point loading was applied. For more details, the geometry and loading conditions are given in Fig. 2.

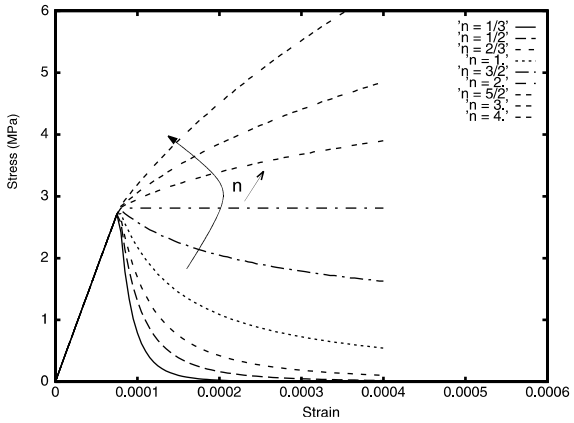


Fig. 1. Influence of the exponent parameter $n$ on the stress–strain behaviour.

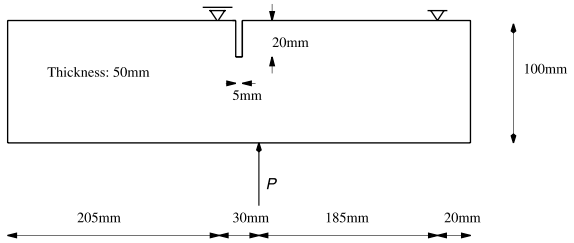


Fig. 2. Single-edge notched beam. Geometry and loading configuration.

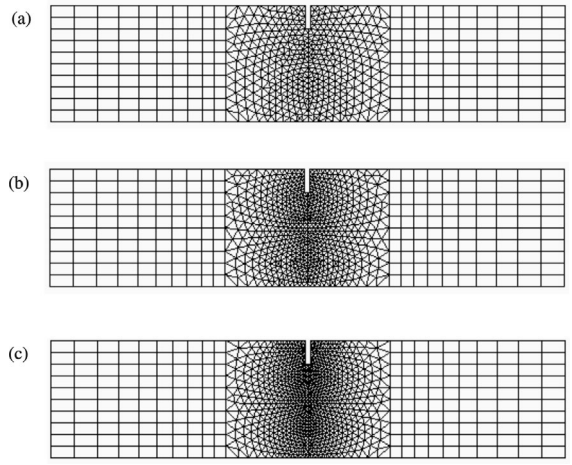


Fig. 3. Finite element discretizations of the single-edge notched beam.

To show the lack of mesh sensitivity of the damage modelling framework used in this paper, the computations are carried out with three different finite element meshes given in Fig. 3. The mesh (a) contains 950 elements (750 triangles and 200 quadrilaterals), the mesh (b) contains 1466 elements (1266 triangles and 200 quadrilaterals), and the mesh (c) contains 1970 elements (1770 triangles and 200 quadrilaterals). Note that for the three meshes, the loadings and the boundary conditions are applied on single node points.

The material parameters used for the numerical computations are: $E = 33,000$ MPa, $\nu = 0.18$, $W = 1.2 \times 10^{-4}$ MPa, $k = 0.02$ MPa mm$^2$ and $n = 0.9$ (softening). Loading is performed by controlling the vertical displacement of the node where the force $P$ is applied. The three 'Force $P$ versus the vertical displacement $d$' curves corresponding to the three meshes are plotted in Fig. 4. One can note the objectivity of these results with regards to the global behaviour of the structure.

To illustrate the lack of mesh sensitivity at the local level, we show the computed damage fields obtained with the three meshes at two different loading situations. Fig. 5 shows the damage fields corresponding to the vertical displacement $d = 0.0525$ mm, and Fig. 6 shows the ones corresponding to the vertical

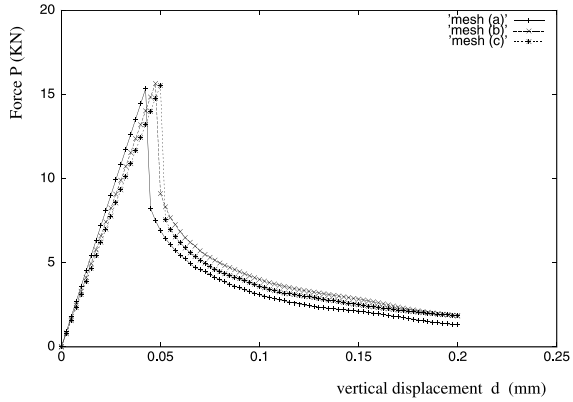


Fig. 4. Force $P$ versus vertical displacement $d$ for the three meshes.

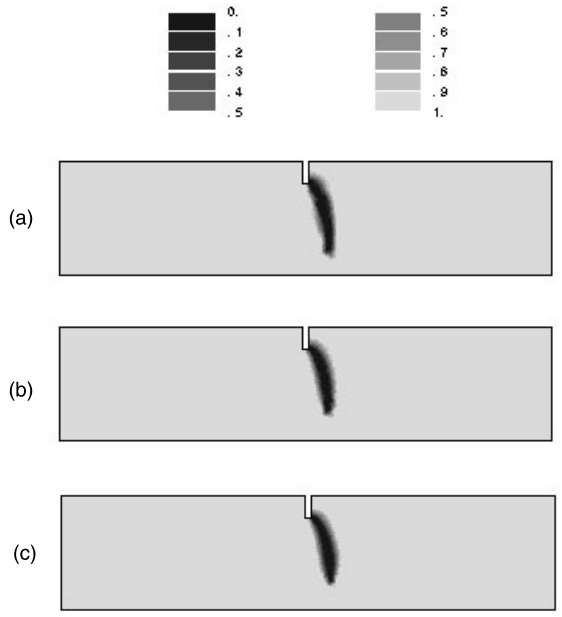


Fig. 5. Damage fields at vertical displacement $d = 0.0525$ mm for the three meshes.

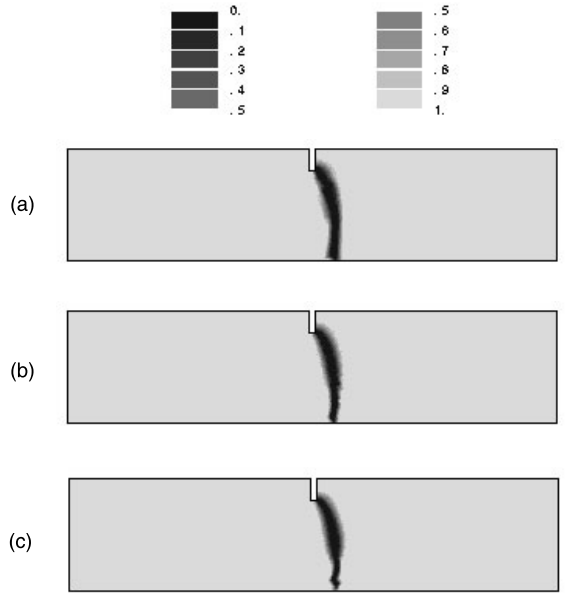


Fig. 6. Damage fields at vertical displacement $d = 0.2$ mm for the three meshes.

displacement $d = 0.2$ mm (see Fig. 4). One can see that damage initiates at the right corner of the notch and ends at the location of the point load $P$.

This (nonhomogeneous) example also shows the role exhibited by the activation of the factor of influence of damage $k$ to control the width of the damaged zone. Furthermore the dissymmetric behaviour (between tension and compression) predicted by the elastic-damage model of Section 3 is clear (see Remark 1).

### 6.3. Elastoplastic-damage with associative $J_2$ plasticity

In this section, the model example of Section 4.2 is extended to include *non-linear* hardening in the plastic modelling part. While the damage part remains unchanged, nonlinear isotropic and kinematic hardening rules are included in the plastic part which are specified by means of a hardening parameter and a plastic modulus for the back stress. These parameters are in turn assumed to be arbitrary functions of the equivalent plastic strain. We refer to Simo and Hughes (1998) and Simo and Taylor (1985) for a complete detail about this specific plastic model.

Consistent with the present elastoplastic-damage framework, the plastic part is given directly in the standard format (see Remark 7). The pressure insensitive yield criterion, in place of Eq. (50), is given by:

$$f(\boldsymbol{\zeta}, \boldsymbol{\chi}, \kappa; \beta) = \frac{\|\boldsymbol{\zeta}\|}{\beta} - \sqrt{\frac{2}{3}}\kappa(e^{\mathrm{p}}) \leqslant 0, \tag{70}$$

$$e^{\mathrm{p}} = \int_0^t \sqrt{\frac{2}{3}}\|\dot{\boldsymbol{\epsilon}}^{\mathrm{p}}(\tau)\|\,\mathrm{d}\tau, \qquad \boldsymbol{\zeta} = \mathrm{dev}[\boldsymbol{\sigma}] - \boldsymbol{\chi}, \tag{71}$$

where $\boldsymbol{\chi}$ is the back stress, $e^{\mathrm{p}}$ is the equivalent plastic strain and $e^{\mathrm{p}} \rightarrow \kappa(e^{\mathrm{p}})$ is the hardening rule. Here $\boldsymbol{\chi}$ and $\kappa(e^{\mathrm{p}})$ play the role of the internal (stress-like) plastic variable $\mathbf{q}$ specified in the general theory of Section 4. The rest of the evolution equations are given as follows:

$$\dot{p} = \frac{1}{3}\mathrm{tr}[\dot{\boldsymbol{\sigma}}] = \beta\left(\lambda + \frac{2}{3}\mu\right)\mathrm{tr}[\dot{\boldsymbol{\epsilon}}], \qquad \mathrm{dev}[\dot{\boldsymbol{\sigma}}] = 2\beta\mu(\mathrm{dev}[\dot{\boldsymbol{\epsilon}}] - \dot{\boldsymbol{\epsilon}}^{\mathrm{p}}), \tag{72}$$

$$\dot{\boldsymbol{\chi}} = \frac{2}{3}\beta H'_{\alpha}(e^{\mathrm{p}})\dot{\boldsymbol{\epsilon}}^{\mathrm{p}}, \qquad \dot{\boldsymbol{\epsilon}}^{\mathrm{p}} = \dot{\gamma}\frac{\partial f}{\partial \boldsymbol{\zeta}} = \bar{\mathbf{n}}, \tag{73}$$

where $H'_{\alpha}(e^{\mathrm{p}})$ is the plastic modulus and $\bar{\mathbf{n}} = \boldsymbol{\zeta}/\|\boldsymbol{\zeta}\|$ is the unit normal to the yield surface. For the nonlinear functions $\kappa(e^{\mathrm{p}})$ and $H_{\alpha}(e^{\mathrm{p}})$ we take, as in Simo and Hughes (1998) and Simo and Taylor (1985):

$$\delta\kappa(e^{\mathrm{p}}) + (1-\delta)H_{\alpha}(e^{\mathrm{p}}) = Y_{\infty} - [Y_{\infty} - Y_0]\exp[\ell e^{\mathrm{p}}] + \bar{Y}e^{\mathrm{p}}, \quad \delta \in [0,1], \tag{74}$$

where $\delta = 0$ and $\delta = 1$ correspond to the limit cases of pure kinematic and pure isotropic hardening rules, respectively.

Fig. 7 shows the result of an uniaxial tension test computed by using the following material parameters: $E = 35,000$ MPa and $\nu = 0.18$ for elasticity, $W = 0.48 \times 10^{-4}$ MPa and $n = 2/3$ for the damage part, and $Y_0 = 2.8$ MPa, $Y_{\infty} = 3.2$ MPa, $\ell = 0.15$, $\bar{Y} = 125$ MPa and $\delta = 0.8$ for the plastic part. The value of $k$ is not given for instance because of the homogeneous deformation state.

As expected, we see from the unloading path that plasticity is accompanied by a loss of stiffness (damage).

The present model is used to compute the double notched specimen shown in Fig. 8. This is carried out with the three finite element meshes given in Fig. 9. For obvious symmetry reasons, only 1/4 of the specimen needs to be considered. The mesh (a) contains 318 elements, the mesh (b) contains 1001 elements and the mesh (c) contains 1472 elements.

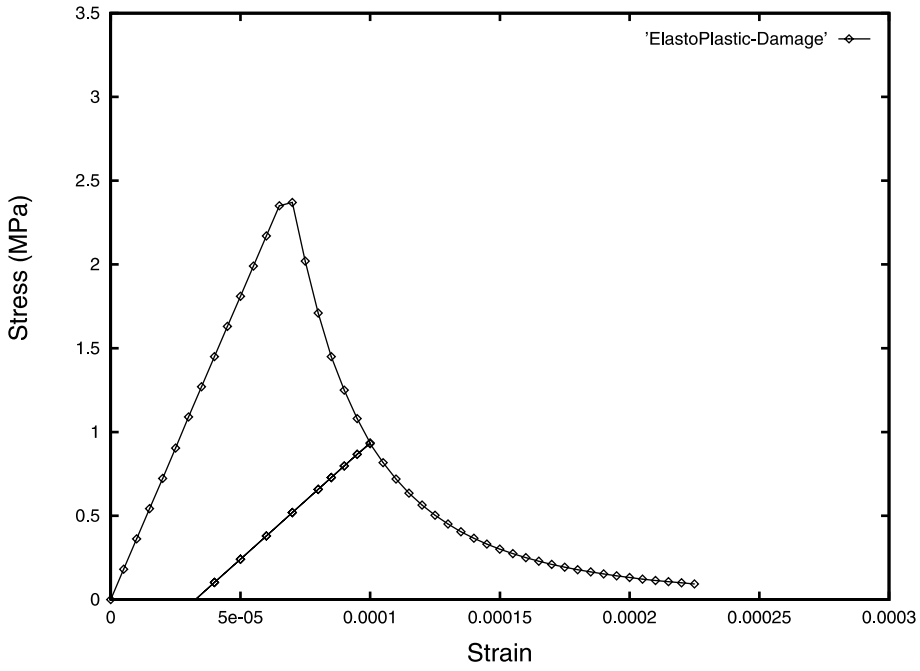


Fig. 7. Uniaxial stress–strain behaviour with $J_2$ plasticity.

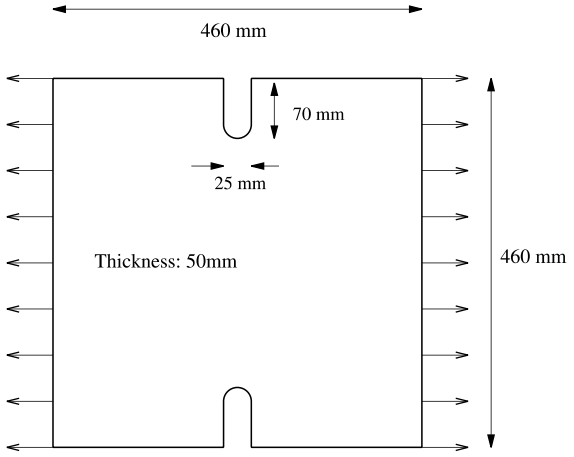


Fig. 8. The double notched specimen. Geometry and loading configuration.

The material parameters used for the computations are those of Fig. 7 with, in addition, the factor of influence of damage $k = 0.15$ MPa mm$^2$.

Loading is performed by controlling the horizontal displacements of the left boundary. The three 'Load versus horizontal displacement' curves corresponding to the three meshes are plotted in Fig. 10. One can note the objectivity of these results with regards to the global behaviour of the structure.

To illustrate the good performance of the model with regards to the mesh sensitivity at the local level, we compare the damage fields and the elastic–plastic interfaces for the three meshes at the same load level. For

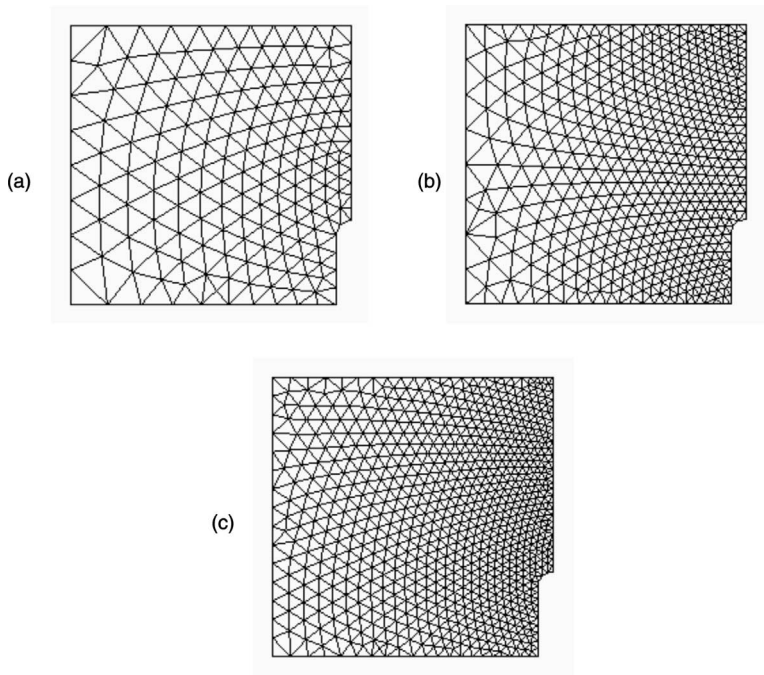


Fig. 9. Finite element discretizations of the double notched specimen.

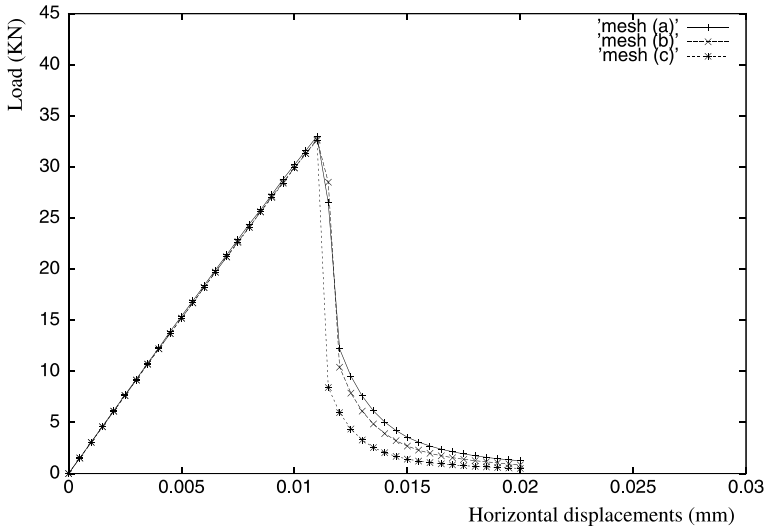


Fig. 10. Load versus horizontal displacement for the three meshes.

this, we choose to show these computed results at the imposed horizontal displacement (load level) $h = 0.02$ mm, which, as shown in Fig. 10 corresponds to a quasi-complete failure of the specimen.

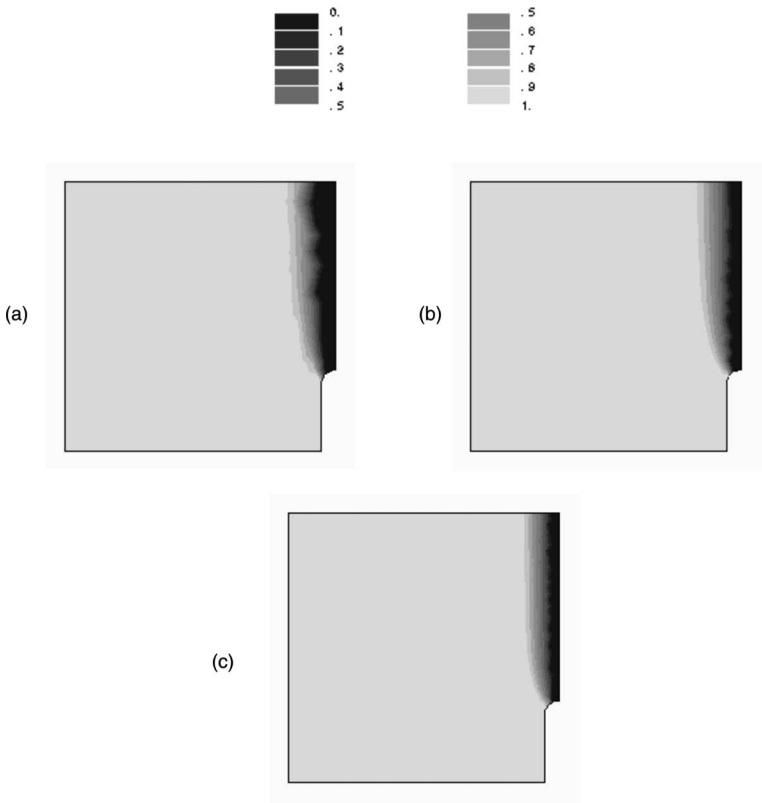


Fig. 11. Damage field at the horizontal displacement $h = 0.02$ mm.

Fig. 11 shows the damage fields for the three meshes, and Fig. 12 shows the corresponding elastic–plastic interfaces. Note that for this last result (Fig. 12), the plotting is accomplished directly from the Gauss points of a typical element and no *smoothing* procedure is performed.

### 6.4. An example with rate-dependent damage and rate-dependent plasticity

In this section, we illustrate through a model example the extension of the preceding developments to incorporate rate-dependent response (visco-damage and/or viscoplasticity). For the damage part of the modelling, visco-damage is introduced simply by using the rate-dependent version of the model outlined in Section 3, i.e. with the viscosity parameter of damage $c \neq 0$. For the plastic part however, viscoplasticity can be introduced by using, for example, a Perzyna type model of evolution.

To make matters as concrete as possible, let us use for the plastic part a simplified version of the model described in the last example, namely, a $J_2$-flow plasticity with linear isotropic hardening. In this case, the pressure insensitive yield criterion is given by,

$$f(\boldsymbol{\sigma}, e^{\mathrm{p}}; \beta) = \frac{\|\mathrm{dev}[\boldsymbol{\sigma}]\|}{\beta} - \sqrt{\frac{2}{3}}(Y_0 + \bar{Y} e^{\mathrm{p}}) \leqslant 0, \tag{75}$$

where $e^{\mathrm{p}}$ is the equivalent plastic strain, $Y_0$ is the effective flow stress and $\bar{Y}$ the effective plastic modulus. The evolution equations are those given by Eq. (72) together with

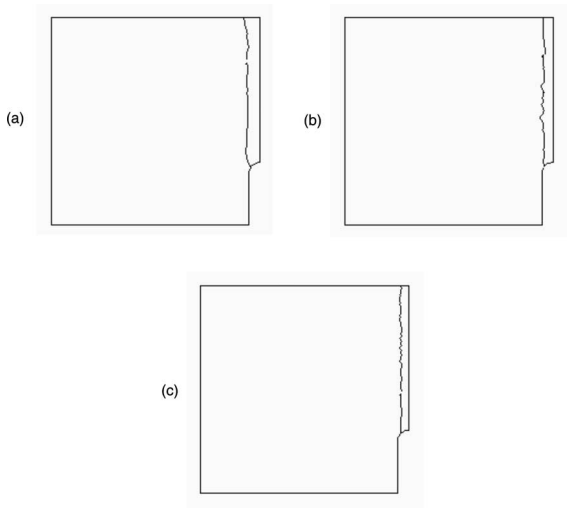


Fig. 12. Elastic–plastic interface at the horizontal displacement $h = 0.02$ mm.

$$\begin{cases} \dot{\boldsymbol{\epsilon}}^{\mathrm{p}} = \dot{\gamma}\bar{\mathbf{n}}, \quad \bar{\mathbf{n}} = \frac{\mathrm{dev}[\boldsymbol{\sigma}]}{\|\mathrm{dev}[\boldsymbol{\sigma}]\|}, \\ \dot{e}^{\mathrm{p}} = \sqrt{\frac{2}{3}}\dot{\gamma}, \end{cases} \tag{76}$$

with the difference that for viscoplasticity, the Kuhn–Tucker loading/unloading conditions are replaced by the constitutive equation:

$$\dot{\gamma} = \frac{1}{\eta}\ \langle g(f(\boldsymbol{\sigma}, e^{\mathrm{p}}; \beta))\rangle^{+}, \tag{77}$$

with $g(x) \geqslant 0\ \forall x \in \mathbb{R}^{+}$ and $g(x) = 0 \Longleftrightarrow x = 0$, and where we recall that $\langle\cdot\rangle^{+}$ is the positive part of $\langle\cdot\rangle$. This relation defines a penality regularization of the rate-independent version with plastic viscosity constant $\eta \in [0, \infty[$. In what follows, the general function $g$ in Eq. (77) is replaced by the identity, $g(x) = x$.

From the algorithmic point of view, visco-damage is treated at the global level by adding the term corresponding to $c\dot{\beta}$ (see first term of Eq. (14)) and then by performing an implicit backward-Euler scheme before the linearization procedure described in Section 5.2. At the local level, viscoplasticity is accommodated by standard algorithms. The local algorithm we use for this is the one described in detail in Simo and Hughes (1998), which circumvents the characteristic ill-conditioning exhibited in the rate-independent limit as the plastic viscosity $\eta \to 0$.

The present rate-dependent model is used to compute the tensions of the double-edge notched specimen shown in Fig. 13 at different loading velocities. The specimen is fixed horizontally and vertically at the bottom, and at the top side, it is fixed horizontally and loaded in tension vertically. The finite element discretization we use is also shown in Fig. 13. It contains 812 four-nodes quadrilateral elements. During the computations, loading is performed by controlling the vertical displacements of the top side of the specimen.

The material parameters used for the computations are: $E = 35,000$ MPa and $\nu = 0.2$ for elasticity, $W = 0.52 \times 10^{-4}$ MPa, $n = 1$, $k = 0.05$ MPa mm$^2$ and $c = 0.35 \times 10^{-2}$ MPa s for the damage part, and $Y_0 = 2.2$ MPa, $\bar{Y} = 135$ MPa and $\eta = 225$ MPa s for the plastic part.

Fig. 14 shows the 'resultant applied force versus imposed vertical displacement at the top face' curves obtained for different loading velocities. These curves are plotted together with the one obtained with the

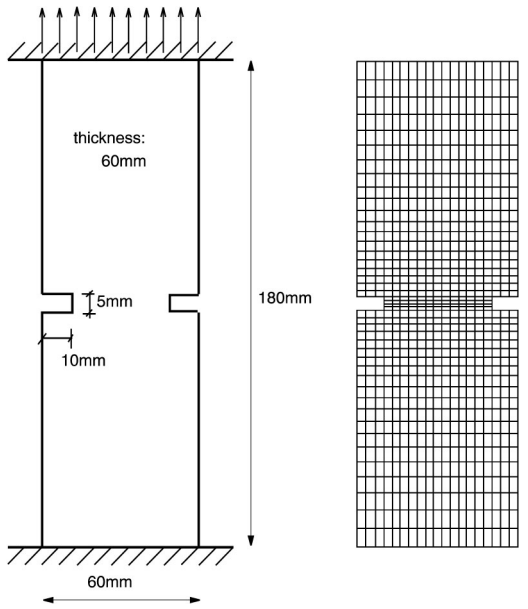


Fig. 13. Tension of a double-edge notched specimen. Geometry, loading configuration and finite element discretization.

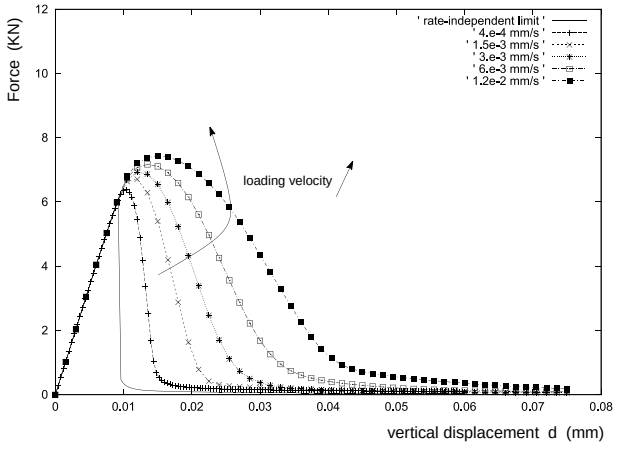


Fig. 14. Resultant force versus imposed vertical displacement for different loading velocities. Comparison with the rate-independent version of the model.

inviscid version of the model, i.e. with rate-independent damage, $c = 0$, and rate-independent plasticity, $\eta = 0$.

Inspection of these results clearly shows the role exhibited by the presence of viscosity in the behaviour of the constitutive material. On one hand, as the loading velocity increases, the maximum load carrying capacity of the specimen increases and the softening part of the response is delayed. And on the other hand, as the loading velocity decreases, the response of the specimen tends to the one obtained with the rate-independent version of the model.

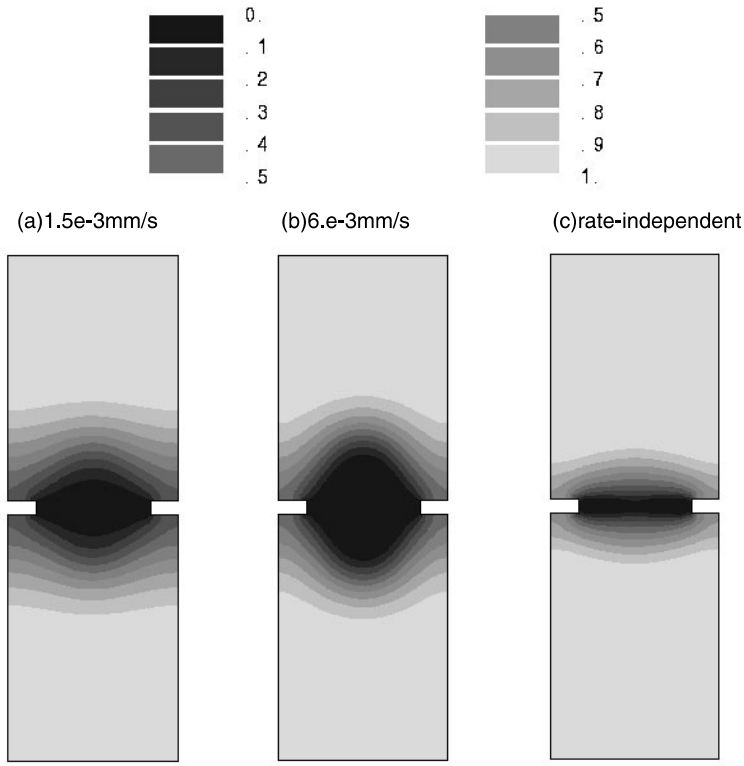


Fig. 15. Damage fields at $d = 0.075$ mm for the loading velocities: (a) $\dot{\bar{u}} = 1.5 \times 10^{-3}$ mm/s and (b) $\dot{\bar{u}} = 6 \times 10^{-3}$ mm/s. Comparison with the corresponding rate-independent version in (c).

To show the influence of the loading velocity on the local response of the specimen, we choose to show in Fig. 15 the computed damage fields obtained at the imposed vertical displacement $d = 0.075$ mm for the two different loading velocities: (a) $\dot{\bar{u}} = 1.5 \times 10^{-3}$ mm/s, and (b) $\dot{\bar{u}} = 6 \times 10^{-3}$ mm/s (see Fig. 14). As a comparison, these results are plotted together with the corresponding damage field obtained with the rate-independent version of the model in Fig. 15(c).

From these last results at the local level, a noteworthy remark should be addressed. In fact, we observe that the area of the completely damaged zone increases with increasing loading velocity. At the limiting case of a very small loading velocity, this area tends to the one shown in Fig. 15(c).

### 6.5. Elastoplastic-damage with non associative plastic flow

Here the elastic-damage model of Section 3 is coupled with the non associative plastic flow model described in detail in Simo and Taylor (1985). For the plastic part, we consider the following, Drucker–Prager type, pressure sensitive yield criterion:

$$f(\boldsymbol{\sigma};\beta) = \|\mathrm{dev}[\boldsymbol{\sigma}]\| - \sqrt{\frac{2}{3}}\kappa(p;\beta), \tag{78}$$

$$p = \frac{1}{3}\mathrm{tr}[\boldsymbol{\sigma}], \qquad \kappa(p;\beta) = \beta\bar{c} - \tan(\phi)p, \tag{79}$$

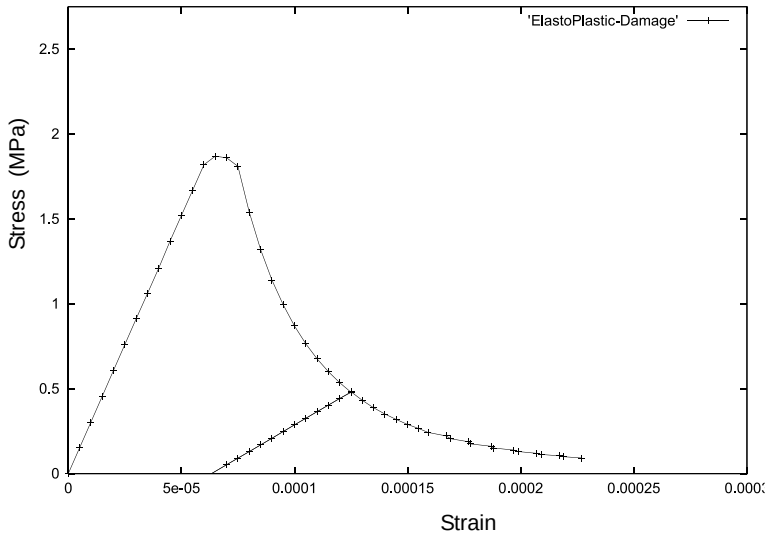


Fig. 16. Uniaxial stress–strain behaviour with Drucker–Prager type plastic model.

where $\bar{c}$ and $\phi$ are here material parameters. In soil mechanics, $\bar{c}$ stands for the cohesive stress and $\phi$ refers to the friction angle. As in Simo and Taylor (1985), we consider the case in which the plastic flow is pressure insensitive:

$$\dot{\boldsymbol{\epsilon}}^{\mathrm{p}} = \dot{\gamma}\bar{\mathbf{n}}, \quad \text{with } \bar{\mathbf{n}} = \frac{\mathrm{dev}[\boldsymbol{\sigma}]}{\|\mathrm{dev}[\boldsymbol{\sigma}]\|}. \tag{80}$$

Fig. 16 shows the result of an uniaxial test computed by using the following material parameters: $E = 27,000$ MPa and $\nu = 0.333$ for elasticity, $W = 0.4 \times 10^{-4}$ MPa and $n = 2/3$ for the damage part, and $\bar{c} = 2.4$ MPa and $\tan(\phi) = 0.879$ for the plastic part. Here also the value of $k$ is not specified because of the homogeneous deformation state.

As for the model example Section 6.3 (Fig. 7), we see from the unloading path that plasticity is accompanied by a loss of stiffness (damage).

### 6.6. Another elastoplastic-damage model

Other models can also be investigated. One can think, for example, of models where damage is produced by plasticity, i.e. metals for example, or models where plasticity (or permanent deformation) is produced by damage, i.e. rock-like materials for example.

In this section, we give a simple model example of the first type (damage produced by plasticity) as follows.

We choose the plastic part of the modelling to be characterized by the $J_2$-flow plastic model (coupled with damage) of Section 6.3, which is described by the definitions and evolution Eqs. (70)–(74).

For the damage part of the modelling a little adaptation is introduced. As a source of damage, instead of the strain energy $S(\boldsymbol{\epsilon})$ given by Eq. (12) (in the expression of $\Phi^{\mathrm{ed}}$, Eq. (49)), we use an energy governed by the plastic strains $S(\boldsymbol{\epsilon}^{\mathrm{p}})$ (see first term in Eq. (53)). In this example, we use the following simple expression:

$$S(\boldsymbol{\epsilon}^{\mathrm{p}}) = \mu_{\mathrm{p}}\boldsymbol{\epsilon}^{\mathrm{p}} : \boldsymbol{\epsilon}^{\mathrm{p}}, \tag{81}$$

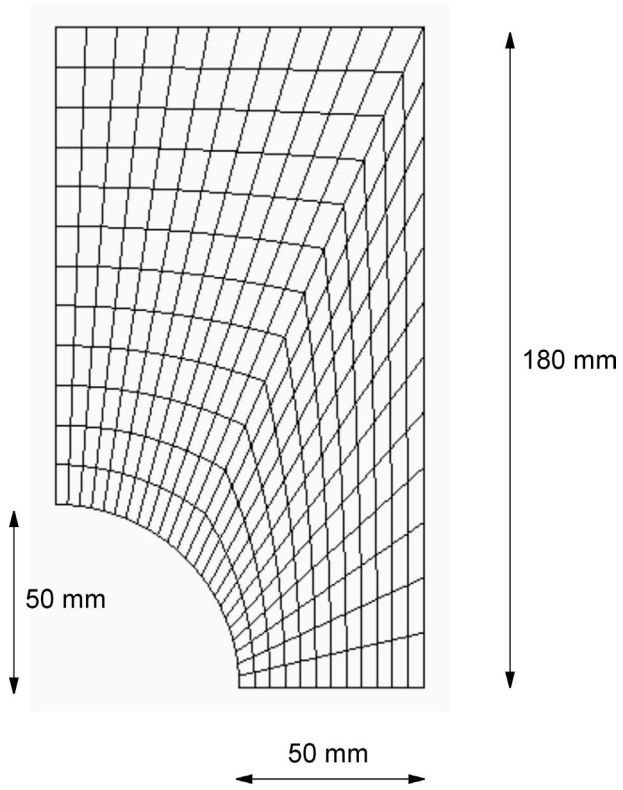


Fig. 17. Perforated strip. Finite element mesh (288 elements).

where $\mu_p$ is a material parameter. Note that, following the same philosophy of this modelling type, we can alternatively use a function of the equivalent plastic strain $S(e^p)$ in place of $S(\epsilon^p)$ in Eq. (81).

As an application of the present model, we consider the plane strain problem of a rectangular strip with a circular hole, subjected to increasing extension in a direction perpendicular to the axis of the strip and parallel to one of its sides. Loading is performed by controlling the vertical displacement of the top and bottom boundaries. The finite element mesh employed is shown in Fig. 17. For obvious symmetry reasons, only 1/4 of the strip needs to be considered.

The material parameters used for the computation are: $E = 35,000$ MPa and $\nu = 0.3$ for elasticity, $W = 3.25 \times 10^{-4}$ MPa, $n = 0.8$, $k = 0.1$ MPa mm$^2$ and $\mu_p = 21,500$ MPa for the damage part, and $Y_0 = 2.2$ MPa, $Y_\infty = 3.25$ MPa, $\ell = 6.75$, $\bar{Y} = 2500$ MPa and $\delta = 1.$ for the plastic part. With these parameters, the resulting stress–strain behaviour in tension is shown in Fig. 18.

The evolution of the elastic–plastic interface with increased straining of the strip is shown in Fig. 19 for the following three loading situations: (a) at imposed vertical displacement $d = 0.01$ mm, (b) at $d = 0.02$ mm, and (c) at $d = 0.03$ mm. Fig. 19(a) shows that plasticity starts from the parts of the hole whose normals are perpendicular to the loading direction, and grows to reach the external vertical sides of the strip (Fig. 19 (b) and (c)).

In Fig. 20 we show the damage fields corresponding to the loading situations of Fig. 19. Inspection of Fig. 20(a) shows that while plasticity is taking place (Fig. 19(a)), the damage process has not started. This is in accordance with the present model since the damage growth takes place only when a certain threshold of plasticity is reached. In Fig. 20(b) and (c), the damage process takes place because plasticity is large enough.

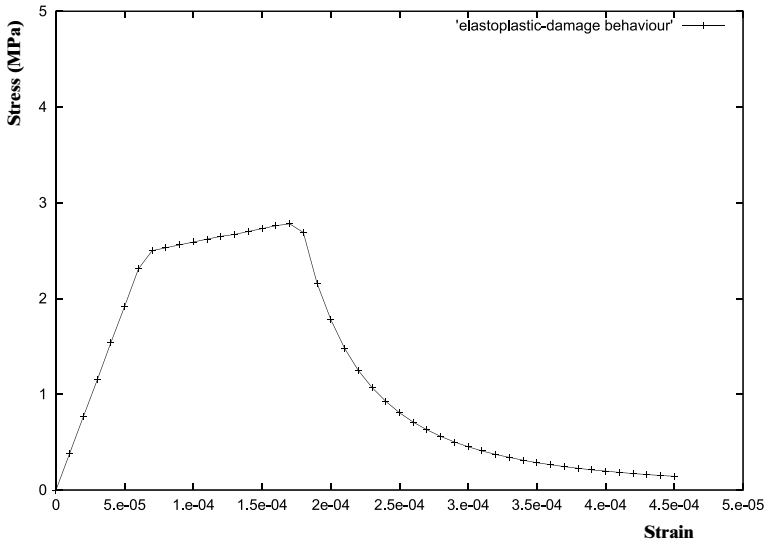


Fig. 18. Stress–strain behaviour used for the perforated strip.

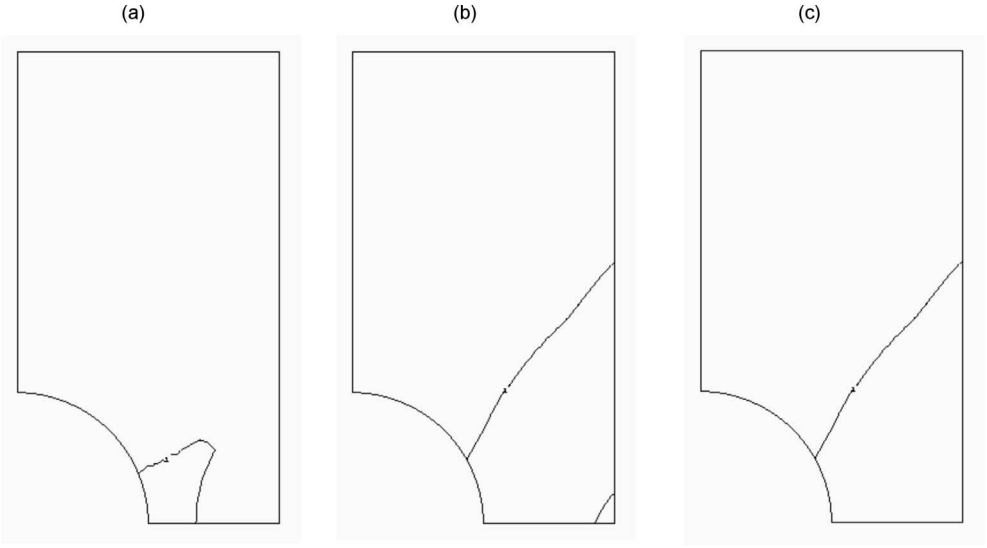


Fig. 19. Elastic–plastic interface at: (a) $d = 0.01$ mm, (b) $d = 0.02$ mm, (c) $d = 0.03$ mm.

The damage starts at the parts of the hole whose normal is perpendicular to the loading direction, and grows horizontally to reach the external sides.

Finally, by comparing the results of Figs. 19 and 20, we clearly see that the area of the plastic zone is always greater than the one of the corresponding damaged zone. This is another characteristic of the present model resulting from the fact that plasticity always precedes damage.

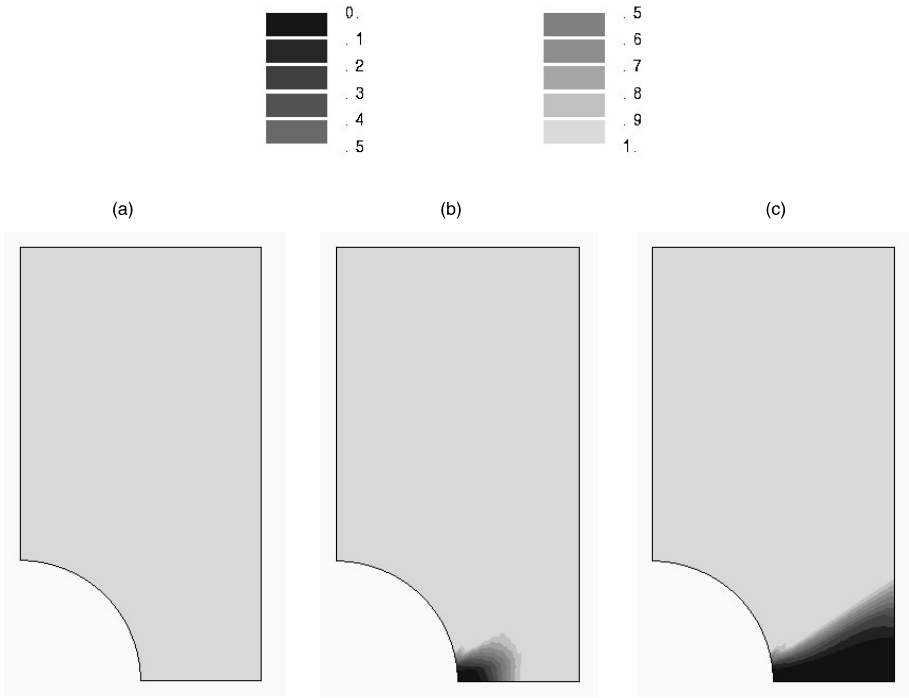


Fig. 20. Damage field at: (a) $d = 0.01$ mm, (b) $d = 0.02$ mm, (c) $d = 0.03$ mm.

## 7. Conclusion

Within the context of a recently proposed formulation of continuum damage mechanics, a framework of elastoplastic-damage modelling has been investigated. The particularity of this damage formulation is that it involves the gradient of damage to take into account the influence of damage at a material point on the damage of its neighbourhood Frémond and Nedjar (1993, 1996) and Nedjar (1995).

Consistent with thermodynamic requirements, it was shown how simple coupling between damage and plasticity can be obtained. In particular, the plastic part of the modelling takes a standard format like in classical elastoplasticity.

The problem of numerically integrating the resulting constitutive equations has been given in detail. It results in an elastic-damage predictor/plastic corrector scheme. The algorithm used for the elastic-damage predictor part is the one already used in Frémond and Nedjar (1993, 1996) and Nedjar (1995, 1999a). Although this algorithm is perfectible (this point is actually under investigation) as pointed out, it gives satisfactory results for the damage evolutions. For the plastic corrector part, classical return mapping is used where a simple coupling with damage is added. From the practical standpoint, the well known closest-point projection and cutting-plane algorithms, see Ortiz and Simo (1986), Simo and Hughes (1987, 1998) and Simo and Taylor (1985) among others, remain unchanged.

For future developments, other models can also be investigated. One can think, for example, of models where damage is produced by plasticity (see the model example of Section 6.5), i.e. metals for example, or models where plasticity (or permanent deformation) is produced by damage, i.e. rock-like materials for example.

## References


Coleman, B.D., Noll, W., 1963. The thermodynamics of elastic materials with heat conduction and viscosity. Arch. Ratio. Mech. Analysis 13, 167–178.

Coleman, B.D., Gurtin, M., 1967. Thermodynamics with internal variables. J. Chem. Phys. 48 (2), 597–613.

Dubé, J.F., Pijaudier-Cabot, G., Laborderie, C., 1994. Rate dependent damage model for concrete in dynamics. ASCE J. Engng. Mech. 122, 639–647.

Frémond, M., Nedjar, B., 1993. Endommagement et principe des puissances virtuelles. C. R. Acad. Sci. Paris, serie II 317, 857–864.

Frémond, M., Nedjar, B., 1996. Damage, gradient of damage and principle of virtual power. Int. J. Solids Struct. 33 (8), 1083–1103.

Germain, P., 1973. Cours de mécanique des milieux continus. Masson et Cie., Paris.

Germain, P., Nguyen, Q.S., Suquet, P., 1983. Continuum thermodynamics. ASME J. Appl. Mech. 50, 1010–1021.

Hughes, T.J.R., 1987. The finite element method. Prentice-Hall, Englewood-Cliffs, NJ.

Humbert, P., 1989. CESAR-LCPC, un code général de calcul par éléments finis. Bull. Liais. Labo. des Ponts et Chaussées 160, 112–116.

Lemaitre, J., Chaboche, J.L., 1988. Mécanique des matériaux solides, second edn. Dunod, Paris.

Lemaitre, J., 1992. A course on damage mechanics. Springer, Berlin.

Moreau, J.J., 1970. Sur les lois de frottement, de viscosité et de plasticité. C. R. Acad. Sci. Paris 271, 608–611.

Nedjar, B., 1995. Mécanique de l'endommagement. Théorie du premier gradient et application au béton. PhD thesis, Ecole Nationale des Ponts et Chaussées, Paris (in french).

Nedjar, B., 1999a. Damage and gradient of damage in transient dynamics, in: Argoul, P., et al., Eds. Proceedings IUTAM'97: variation of Domain and Free-Boundary Problems in Solid Mechanics. Kluwer Academic Publishers, pp. 189–196.

Nedjar, B.,1999b. A framework for elastoplastic-damage models including the gradient of damage. Formulation and computational aspects. Proceedings ECCM'99: European Conference on Computational Mechanics, Munich.

Needleman, A., 1987. Material rate-dependence and mesh sensitivity in localization problems. Comp. Meth. Appl. Mech. Engng. 67, 68–85.

Ortiz, M., Simo, J.C., 1986. An analysis of a new class of integration algorithms for elastoplastic constitutive equations. Int. J. Num. Meth. Engng. 21, 1561–1576.

Peerlings, R.H.J., deBorst, R., Breckelmans, W.A.M., Geers, M.G.D., 1998. Gradient enhanced damage modelling of concrete fracture, Mech. Cohesive-Frictional Mat. 3, 323–342.

Pijaudier-Cabot, G., Burlion, N., 1996. Damage and localization in elastic materials with voids. Mech. Cohesive-Frictional Mat. 1, 129–144.

Schlangen, E., 1993. Experimental and numerical analysis of fracture process in concrete. Dissertation, Delft University of Technology, Delft.

Simo, J.C., 1988. Strain softening and dissipation: A unification of approaches, in: J. Mazars and Bazant, Z.P., (Eds)., Proceedings Cracking and damage, strain localization and size effect, Elsevier, Amsterdam, pp. 440–461.

Simo, J.C., Hughes, T.J.R., 1987. General return mapping algorithms for rate-independent plasticity, in: Desai, C.S., et al., (Eds)., Proceedings Constitutive laws for engineering materials: theory and applications, Elsevier, pp. 221–231.

Simo, J.C., Hughes, T.J.R., 1998. Computational inelasticity. Springer, New York.

Simo, J.C., Ju, J.W., 1987a. Strain- and Stress-based continuum damage models. Part I: Formulation. Int. J. Solids Struct. 23(7), 821–840.

Simo, J.C., Ju, J.W., 1987b. Strain- and Stress-based continuum damage models. Part II: Computational aspects. Int. J. Solids Struct. 23(7), 841–869.

Simo, J.C., Taylor, R.L., 1985. Consistent tangent operators for rate-independent elastoplasticity. Comp. Meth. Appl. Mech. Engng. 48, 101–118.

Zienkiewicz, O.C., Taylor, R.L., 1989. The finite element method, vol. 1,fourth ed. McGraw-Hill, London.